Insight into the compatibility behaviors between various rejuvenators and aged bitumen: Molecular dynamics simulation and experimental validation

Ren, S.; Liu, X.; Lin, P.; Gao, Y.; Erkens, S.

DOI
10.1016/j.matdes.2022.111141

Publication date
2022

Document Version
Final published version

Published in
Materials & Design

Citation (APA)
Ren, S., Liu, X., Lin, P., Gao, Y., & Erkens, S. (2022). Insight into the compatibility behaviors between various rejuvenators and aged bitumen: Molecular dynamics simulation and experimental validation. *Materials & Design*, *223*, Article 111141. https://doi.org/10.1016/j.matdes.2022.111141

Materials & Design 223 (2022) 111141

Contents lists available at ScienceDirect

Materials & Design

journal homepage: www.elsevier.com/locate/matdes

Insight into the compatibility behaviors between various rejuvenators and aged bitumen: Molecular dynamics simulation and experimental validation

Shisong Ren *, Xueyan Liu, Peng Lin, Yangming Gao, Sandra Erkens

Section of Pavement Engineering, Faculty of Civil Engineering & Geosciences, Delft University of Technology, Stevinweg 1, 2628 CN Delft, the Netherlands

HIGHLIGHTS

- A multi-scale method composed of molecular dynamics simulation and experimental validation is developed to estimate the compatibility of rejuvenator-aged bitumen.
- The compatibility potential ranking from molecular dynamics simulation and experimental results is aromatic-oil > bio-oil > naphthenic-oil > engine-oil.
- Thermal behavior of rejuvenators in aged bitumen is strongly related to intermolecular interaction strength, molecular dispersion, and molecular mobility.
- Aromatic-oil and engine-oil display the strongest and weakest interaction strength with bitumen, but molecular distribution level presents an opposite trend.

GRAPHICAL ABSTRACT

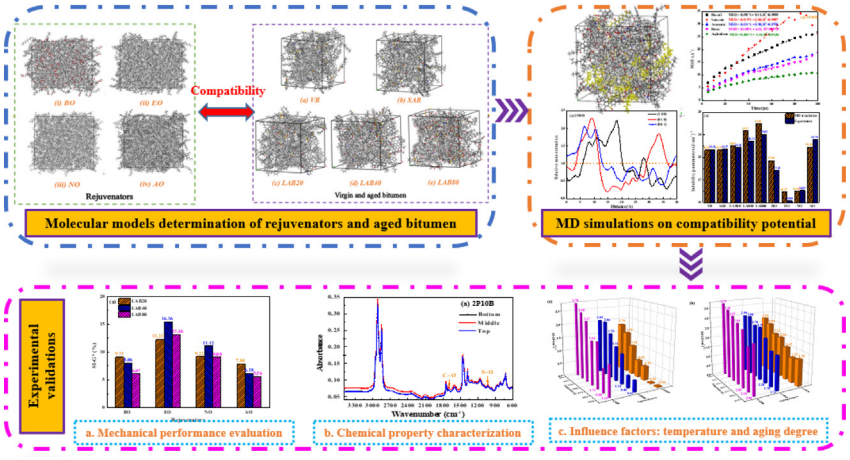

ARTICLE INFO

Article history:
Received 24 April 2022
Revised 4 September 2022
Accepted 8 September 2022
Available online 14 September 2022

Keywords:
Rejuvenator
Aged bitumen
Compatibility
Thermal phase stability
MD simulations

ABSTRACT

The compatibility potential of rejuvenators plays an important role in improving the blending degree of rejuvenated bitumen. This study aims at estimating the efficiency of molecular dynamics (MD) simulation in predicting the compatibility between rejuvenators and aged bitumen, and exploring the influence of rejuvenator type, aging degree of bitumen, and temperature on the compatibility potential. The thermal storage stability of rejuvenated binders is evaluated to validate the compatibility prediction. Afterward, the underlying mechanism for the storage stability difference between rejuvenators and aged bitumen is explained with the atomic-scale parameters. The results revealed that the ranking on predicted compatibility and experimentally measured thermal storage stability for four rejuvenators is the same as AO > BO > NO > EO. Furthermore, the thermodynamic parameters of solubility parameter difference Δδ, Flory-Huggins parameter χ, and mixing free energy ΔGm are efficient for estimating the compatibility potential of various rejuvenators with aged bitumen. Moreover, the separation index (SI) parameters based on rheological and chemical indices are available to assess the phase stability of

* Corresponding author.
E-mail address: Shisong.Ren@tudelft.nl (S. Ren).

https://doi.org/10.1016/j.matdes.2022.111141

rejuvenated bitumen. At the molecular scale, the compatibility and phase stability issues between rejuvenators and aged bitumen are complicated and related to different aspects of intermolecular interaction, dispersion degree, and molecular mobility.

1. Introduction

The increasing traffic loading and variable environmental conditions result in the limited service life of asphalt pavement and the amount of waste reclaimed asphalt pavement (RAP) materials produced during maintenance and reconstruction processes [1,2]. Because of the remarkable environmental and economic benefits, reusing RAP materials in asphalt road construction attracts more attention from pavement researchers [3]. However, it is challenging to recycle the RAP materials in abundance because of the embrittlement and cracking characteristics of the aged binder [4,5].

Lots of studies revealed that the aging mechanism of bitumen is complicated and mainly composed of light-components evaporation, mass conversion from maltene phase to asphaltene fraction, and generation of oxygen-containing functional groups in bitumen molecules [6–8]. All these factors increase bitumen's stiffness, viscosity, and cracking potential [9]. Rejuvenators with light molecular weight often balance the maltene/asphaltene ratio and weaken the influence of polar functional groups [10]. The positive effects of different rejuvenators on restoring and improving the cracking resistance, moisture insensitivity, fatigue life, and anti-aging performance of aged bitumen are reported. However, the adverse effect of their softening characteristics on rutting resistance is also observed [11–13]. All of these evaluations are based on a hypothesis that the rejuvenators have been completely blended with aged bitumen, and a homogeneous rejuvenated bitumen is fabricated [14].

In practical engineering, it is impossible to dissolve all aged bitumen from the RAP and mixed with rejuvenators to obtain the homogenous rejuvenated binder [15]. Instead, the rejuvenators are directly incorporated into an asphalt mixture containing RAP with a mechanical mixing process for a blending duration at high temperatures [16]. It is expected that the RAP aggregates are fully and evenly covered by rejuvenators, which can diffuse quickly and disperse uniformly in aged bitumen to ultimately form a homogeneous rejuvenated bitumen layer outside of all RAP aggregates [17].

However, it is difficult to achieve this goal within a limited period, and partial blending does exist in recycled mixtures, which are strongly dependent on the rejuvenator type, RAP content, aging degree of bitumen, warm-mix additives, mixing temperature and time [18–20]. The unknown and insufficient blending level between the RAP binder with rejuvenators and virgin bitumen makes the agencies limit the amount of RAP aggregates in new asphalt roads [21]. The non-homogeneous dispersion of rejuvenators in recycled asphalt pavement increased the rutting and cracking potential due to the excessively high and low dosage of rejuvenators in various aged bitumen layers [22]. Thence, it is essential to understand the blending mechanism and find more efficient rejuvenators with high blending potential with RAP binders.

Currently, the blending degree between the fresh and aged bitumen has been evaluated by different methods, such as stage extraction [23], microscopic observation [24], and Fourier transform infrared (FTIR) microscopy [25]. Moreover, the improvement effects of rejuvenators on the blending level between fresh and RAP binders have been proved, which strongly depends on the rejuvenator type [26]. The interaction level between the blending interaction between rejuvenators and RAP bitumen is always estimated through a diffusion coefficient parameter [27,28]. The ultimate blending degree of rejuvenated bitumen is attributed to the diffusive rate and compatibility behavior between the rejuvenator and RAP binder. Bad compatibility would result in the inhomogeneous dispersion and phase separation of rejuvenators in aged bitumen, thus increasing the distress occurrence potential of recycled asphalt roads [29,30]. However, few studies focus on the compatibility issue between the rejuvenator and aged bitumen. The variety of rejuvenator types also makes it difficult to figure out the connections between their chemical components and the compatibility potential with RAP bitumen. On the other hand, although the glass transition temperature, rheological indices, solubility parameter, and storage stability index have been adopted to evaluate the compatibility level between the aged bitumen and rejuvenators, the underlying mechanism is still unclear from the viewpoint of intermolecular interactions. It brings challenges in explaining compatibility behaviors between various kinds of rejuvenators with aged bitumen, and thus the development of more efficient rejuvenators with superior compatible capacity is impeded.

The molecular dynamics (MD) simulation method is widely adopted in bituminous materials to explore the interaction mechanism of the bulk [31] and interfacial [32] systems at an atomic level. The storage stability and compatibility of different polymers (such as styrene–butadienestyrene [33], polyethylene [34], epoxy [35], etc.) in bitumen have been investigated based on the solubility parameters and free energy theory [36]. In addition, the MD simulation is successfully employed in estimating the compatibility of polymer blend systems [37,38]. Similarly, Zhang et al. qualified the compatibility of soybean-oil and aged bitumen with MD simulations and softening point difference. It was found that the soybean-oil rejuvenated bitumen exhibited excellent storage stability and compatibility potential [39].

However, the compatibility behaviors between rejuvenators in different categories and aged binders with variable aging levels have not been studied yet. Meanwhile, it is necessary to estimate the efficiency of MD simulations in quantitatively predicting the compatibility degree of rejuvenators in aged binders, which should then be validated and connected with several indicators from laboratory tests. Therefore, this study aims to propose a multi-scale method for evaluating the compatibility between rejuvenators and aged binders. Meanwhile, the effects of rejuvenator types, aging degree of bitumen, and temperature on the compatibility degree have been investigated. Lastly, the underlying mechanism of compatibility difference between different rejuvenator-aged bitumen systems has been fundamentally explored and discussed from an intermolecular interaction viewpoint, molecular mobility and molecular dispersion levels.

2. Research methodology and protocol

Fig. 1. illustrates the detailed research methodology, and the details are introduced as follows: (i) After determining and validating the molecular models of aged binders and rejuvenators, an MD simulation was adopted to predict the cohesive energy density

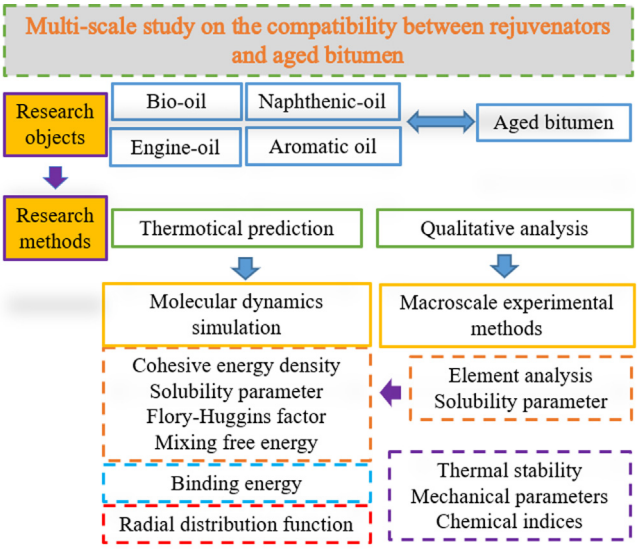

Fig. 1. Research scheme for this study.

(CED) and solubility parameter values. (ii) At the same time, the elemental analysis results are used to calculate the solubility parameters of aged bitumen and rejuvenators, which are compared with MD simulation outputs. (iii) Afterward, three thermodynamics parameters of solubility parameter difference (ΔS), Flory-Huggins factor (χ), and mixing free energy (ΔG_m) between various aged bitumen and rejuvenators are calculated using both MD simulations outputs and experimental results to assess their compatibility and blending possibility from the viewpoint of polymer science theory. (iv) In addition, the molecular models of rejuvenated bitumen are established to measure the binding energy and intermolecular force between rejuvenator and aged bitumen molecules. Meanwhile, the molecular distribution and mobility of rejuvenator molecules in rejuvenated bitumen models are predicted from MD simulations to estimate the compatibility between rejuvenators and aged bitumen from the molecular scale. (v) Lastly, the corresponding rejuvenated binders are manufactured and suffered from the thermal storage test to experimentally evaluate the compatibility and thermal storage stability of rejuvenators in aged bitumen, which are utilized to validate the MD simulations' conclusions.

3. Materials and characterization methods

3.1. Materials

This study used the fresh bitumen with 70/100 PEN-grade from Total Nederland N.V. to fabricate the aged and rejuvenated binders. The physical properties and chemical components of fresh bitumen are listed in Table 1. In addition, four types of rejuvenators were selected to restore the chemical, physical and rheological performance of aged binder, including the bio-oil (BO), engine oil (EO), naphthenic oil (NO), and aromatic oil (AO). The basic properties of these rejuvenators are shown in Table 2. Based on the American national center of asphalt technology report, the rejuvenators for aged bitumen recycling are categorized into five groups: paraffinic oils, aromatic extracts, naphthenic oils, triglycerides & fatty acids, and tall oils [40]. Herein, four rejuvenators belonging to various groups are selected for compatibility research. Table 2 indicates that the aromatic-oil shows the highest density, followed by the bio-oil and naphthenic-oil, and the engine-oil has the lowest value. In addition, the sequence for both viscosity and average molecular weight of these four rejuvenators are the same as BO < EO < NO < AO.

3.2. Preparation of aged and rejuvenated bitumen

The fresh bitumen suffers from the Thin-Film Oven test (TFOT, short-term aging) and Pressure Aging Vessel (PAV, long-term aging) to prepare the aged bitumen for different aging durations [41]. Before the long-term aging, all bitumen suffered from the air oxidation and evaporation process in the TFOT test for 5 h at 163℃. Afterward, the short-term aged binders are subjected to the PAV test at 100 ℃ and 2.1 MPa. The long-term aging time varies from 20 to 40 and 80 h for preparing a series of aged binders with different aging degrees. The virgin, short-term aged, and long-term aged bitumen with 20, 40, and 80 h are labeled as VB, SAB, LAB20, LAB40, and LAB80, respectively.

In addition, the rejuvenated bitumen was prepared by mixing the aged bitumen and rejuvenators manually [42]. The 70 g aged bitumen was heated firstly in an oven with 160 ℃ for 30 min to ensure sufficient flowability and mixability. Afterward, the 7 g (10 % by weight) rejuvenator is incorporated and mixed with aged bitumen for 15 min to guarantee a sufficient-blending state. It should be mentioned that the rejuvenated binder is heated during the blending process to hinder the inhomogeneous condition due to the temperature reduction. In total, 12 rejuvenated binders consisting of rejuvenators (BO, EO, NO, and AO) and aged bitumen (LAB20, LAB40, and LAB80) are manufactured for further thermal storage stability tests.

Table 1
Physical and chemical properties of virgin bitumen.

Properties		Value	Test standard
25℃ Penetration (1/10 mm)		91	ASTM D5
Softening point (℃)		48	ASTM D36
135℃ Dynamic viscosity (Pa•s)		0.8	AASHTO T316
25℃ Density (g/cm^3)		1.017	EN 15326
60℃ Density (g/cm^3)		0.996	
Chemical fractions (wt%)	Saturate, S	3.6	ASTM D4124
	Aromatic, A	53.3	
	Resin, R	30.3	
	Asphaltene, As	12.8	
	Colloidal index CI	0.196	

Table 2
Chemical and physical properties of four rejuvenators.

Rejuvenators	Bio-oil	Engine-oil	Naphthenic-oil	Aromatic-oil
Appearance	Pale-yellow liquid	Brown liquid	Transparent-liquid	Dark-brown half-solid
25℃ Density (g/cm^3)	0.911	0.833	0.875	0.994
60℃ Density (g/cm^3)	0.899	0.814	0.852	0.978
25℃ viscosity (cP)	50	60	130	63,100
Flash point (℃)	> 250	> 225	> 230	> 210
Average molecular weight (g/mol)	286.43	316.38	357.06	409.99

3.3. Experimental methods

3.3.1. Elemental analysis

The elemental analysis was conducted on the virgin, short-term aged, long-term aged bitumen, and four rejuvenators using a Vario EL III elemental analyzer from Elementar Corp., Germany. The sulfanilamide is selected as the reference substance to calibrate the elemental analyzer. During the test, about 5–10 mg bitumen or rejuvenator sample was weighed and put in a tin capsule to monitor the element composition of the carbon (C), hydrogen (H), sulfur (S), nitrogen (N), and oxygen (O) through a combustion way.

3.3.2. Pyknometer density test

The density values of all bitumen and rejuvenator specimens were measured with the specific gravity-capillary-stoppered pycnometer method at both 25 and 60℃ to verify the reasonability of molecular models and simulation settings. The density test operation herein follows the standard of EN 15326 [43].

3.3.3. Thermal storage test

In this study, the thermal storage test is performed to examine the compatibility between the rejuvenator and aged bitumen, which is the standard and commonly-used method to assess the compatibility of polymer-modified bitumen [44,45]. The 50 g rejuvenated bitumen was encased in a cylindrical aluminum tube and vertically stored in an oven with a temperature of 163 ℃ for 48 h. After that, the tube specimens are placed in a refrigerator at −20 ℃ for at least 4 h for rapid cooling and hindering the molecular movement [46]. The cooled tube was evenly separated into three sections with the name of top, middle, and bottom for further rheological and chemical characterizations. It should be noted that each piece is heated and blended further to ensure homogeneous stats before tests.

3.3.4. Dynamic shear rheometer (DSR) test

To quantitatively evaluate the separation degree of rejuvenator from aged bitumen, the evenly-divided rejuvenated bitumen specimens (including top, middle, and bottom sections) after standardized thermal storage procedure are all characterized in terms of rheological and chemical properties. Herein, the DSR measurements consist of the frequency sweep (FS), steady-state flow, and multiple stress creep and recovery (MSCR) tests with a parallel plate geometry of 25 mm diameter and 1 mm gap to evaluate the homogenous degree of rejuvenated binders after thermal storage from the viewpoint of diverse rheological indexes.

During the FS test, two temperatures of 30 and 60 ℃ are selected, with the frequency varying from 0.1 rad/s to 100 rad/s (AASHTO M320 [47]). According to the standard of AASHTO TP70 [48], the temperature and stress levels of the MSCR test herein are 52 ℃ and 0.1/3.2 kPa, respectively. In addition, the steady-state flow test was conducted at 60 ℃ with the shear rate increasing from 10^{-3} to 10^{2} s^{-1} [44–46].

3.3.5. Attenuated reflectance-Fourier transfer infrared (ATR-FTIR) spectroscopy

The difference in chemical characteristics of three separated sections of rejuvenated binders after thermal storage is detected through the PerkinElmer ATR-FTIR method (Waltham, MA, USA) [41]. Each specimen was scanned 12 times with the wavenumber scope of 600–4000 cm^{-1} and a fixed instrument resolution of 4 cm^{-1}. It should be mentioned that all samples have the DSR and FTIR tests at least three times to ensure data reliability.

4. Molecular dynamics simulations

4.1. Molecular structures of virgin and aged bitumen

In this study, the molecular compositions of virgin bitumen come from the commonly-used 12-components model proposed by Li and Greenfield [49], which is illustrated in Fig. 2(a). It should be mentioned that one sulfoxide functional group is supplemented on the molecular structure of the Benzobisbenzothiophene, which is detected in our bitumen from the FTIR test [41]. The oxidation aging would lead to the generation of oxygen-containing functional groups (such as carbonyl and sulfoxide) in bitumen molecules. Thus, these polar oxygen-containing functional groups are added to the molecular structures of aromatic, resin, and asphaltene molecules to represent the aged bitumen molecules, as summarized in Fig. 2(b). As the aging degree progresses, the amount of polar oxygen-containing groups increases gradually.

Moreover, the saturate molecules for aged bitumen are the same as the virgin ones because of their less aging sensitivity. Detailed information regarding the virgin and aged bitumen molecules was introduced in previous studies [50–54]. The molecular number of SARA molecules in virgin and aged bitumen models are summarized in Table 3, which has been verified in terms of SARA fractions and functional group distribution by comparing MD model data with experimental results [50].

4.2. Molecular structures of different rejuvenators

The rejuvenators selected in this study are all commonly used for rejuvenating aged binders in RAP materials. Apart from the bio-oil, the other rejuvenators come from the refinery process of crude oil. Thus, it is easily recognized that the molecular components in these rejuvenators are complicated. There are >50 types of molecules in engine-oil, naphthenic-oil, and aromatic-oil rejuvenators, which brings a huge difficulty in building accurate multi-component molecular models of these rejuvenators. Therefore, the average molecular structures of rejuvenators are adopted herein to assess their compatibility level with aged bitumen molecules.

Fig. 3 displays the average molecular structures of four rejuvenators, determined based on the experimental results regarding elemental composition, functional group distribution, and average molecular weight. All detailed information on establishing the average molecular structures of four rejuvenators can be found in our previous paper [55]. Herein, we only discuss the main difference in the average molecular structures of various rejuvenators. The bio-oil shows the unsaturated alkane with a long carbon chain and an ester group, and the engine-oil molecular structure is composed of one cyclohexane and two alkane side chains. On the other hand, the naphthenic-oil and aromatic-oil rejuvenators exhibit the polycyclic structure together with two alkane side chains. Moreover, all polycyclic rings in the naphthenic-oil are saturated, but the aromatic-oil rejuvenator has the specific polyaromatic characteristic of high polarity and aromaticity. The significant difference in the molecular structures between these four rejuvenators would lead to their different compatibility and dissolution capacity with aged bitumen, which will be explored by a combination of MD simulations and experimental methods.

4.3. MD simulation models and operation details

The molecular models of virgin bitumen, aged bitumen, and rejuvenators are built using Materials Studio software with an initial density of 0.1 g/cm^3. The molecular number of fractional molecules in virgin and aged bitumen models are listed in Table 3, and each rejuvenator model consists of 200 molecules. Afterward,

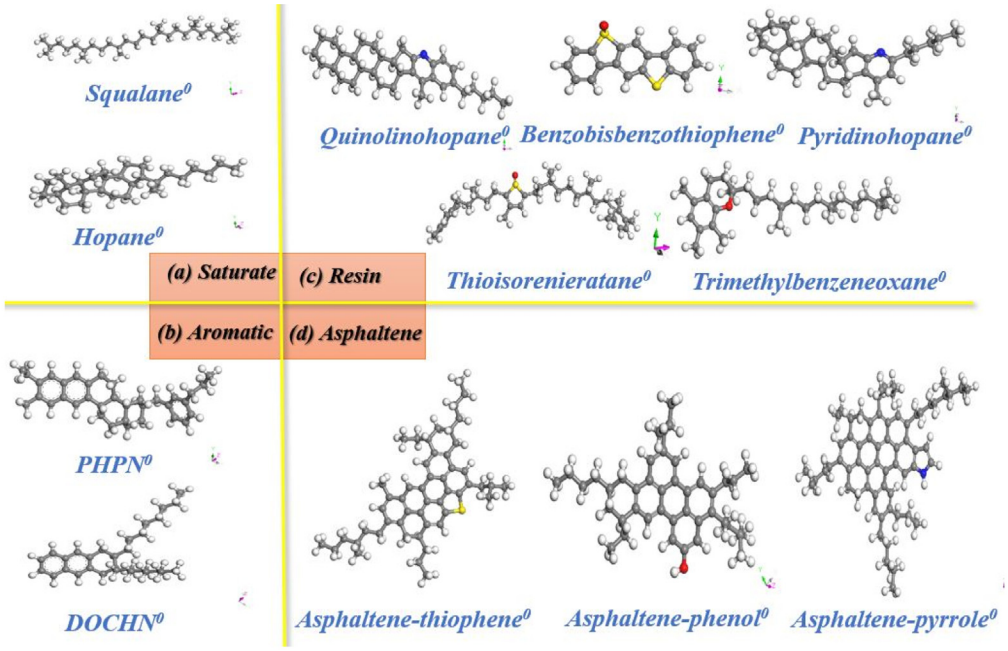

(a) SARA molecules for virgin bitumen

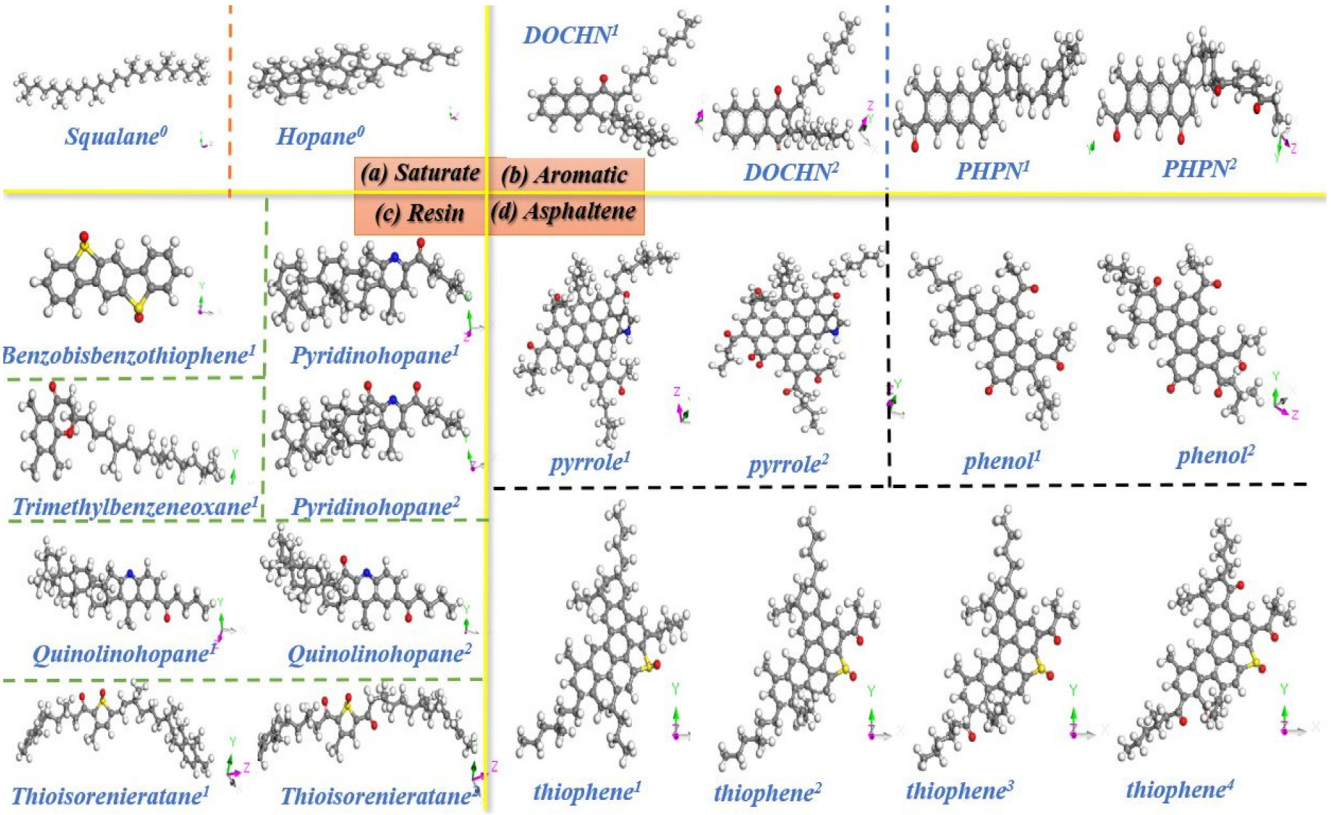

(b) SARA molecules for aged bitumen

Fig. 2. Molecular structures of SARA fractions in virgin and aged bitumen.

geometry optimization is adopted to eliminate the atomic overlap and minimize the system energy. The COMPASSII is a commonly-used force field in organic compounds and bituminous materials. Thus, it is adopted in the whole MD simulations of bitumen and rejuvenator models. The following MD simulation steps are described below:

Table 3
The number of SARA molecules in molecular models of fresh and aged bitumen.

Chemical fractions	Molecular structure	Chemical formula	VB	SAB	LAB20	LAB40	LAB80
Saturate	Squalane^0	$C_{30}H_{62}$	2	2	2	2	2
	Hopane^0	$C_{35}H_{62}$	1	1	1	1	1
Aromatic	PHPN^0	$C_{35}H_{44}$	20	20	12	0	0
	PHPN^1	$C_{35}H_{42}O$	0	0	6	15	0
	PHPN^2	$C_{35}H_{36}O_4$	0	0	0	0	13
	DOCHN^0	$C_{30}H_{46}$	21	20	17	0	0
	DOCHN^1	$C_{30}H_{44}O$	0	0	0	16	0
	DOCHN^2	$C_{30}H_{42}O_2$	0	0	0	0	13
Resin	Quinolinohopane^0	$C_{40}H_{59}N$	3	3	4	0	0
	Quinolinohopane^1	$C_{40}H_{57}NO$	0	0	0	5	0
	Quinolinohopane^2	$C_{40}H_{55}NO_2$	0	0	0	0	5
	Thioisorenieratane^0	$C_{40}H_{60}SO$	3	3	0	0	0
	Thioisorenieratane^1	$C_{40}H_{58}SO_2$	0	0	3	3	0
	Thioisorenieratane^2	$C_{40}H_{56}SO_3$	0	0	0	0	3
	Benzobisbenzothiophene^0	$C_{18}H_{10}S_2O$	13	13	0	0	0
	Benzobisbenzothiophene^1	$C_{18}H_{10}S_2O_2$	0	0	13	14	15
	Pyridinohopane^0	$C_{36}H_{57}N$	3	3	4	0	0
	Pyridinohopane^1	$C_{36}H_{55}NO$	0	0	0	4	0
	Pyridinohopane^2	$C_{36}H_{53}NO_2$	0	0	0	0	5
	Trimethylbenzeneoxane^0	$C_{29}H_{50}O$	4	4	4	5	0
	Trimethylbenzeneoxane^1	$C_{29}H_{48}O_2$	0	0	0	0	6
Asphaltenes	Asphaltene-phenol^0	$C_{42}H_{54}O$	2	2	3	0	0
	Asphaltene-phenol^1	$C_{42}H_{48}O_4$	0	0	0	4	0
	Asphaltene-phenol^2	$C_{42}H_{44}O_6$	0	0	0	0	4
	Asphaltene-pyrrole^0	$C_{66}H_{81}N$	2	2	3	0	0
	Asphaltene-pyrrole^1	$C_{66}H_{73}NO_4$	0	0	0	3	0
	Asphaltene-pyrrole^2	$C_{66}H_{67}NO_7$	0	0	0	0	4
	Asphaltene-thiophene^0	$C_{51}H_{62}S$	2	3	0	0	0
	Asphaltene-thiophene^1	$C_{51}H_{62}SO$	0	0	0	0	0
	Asphaltene-thiophene^2	$C_{51}H_{60}SO_2$	0	0	3	0	0
	Asphaltene-thiophene^3	$C_{51}H_{58}SO_3$	0	0	0	3	0
	Asphaltene-thiophene^4	$C_{51}H_{54}SO_5$	0	0	0	0	4

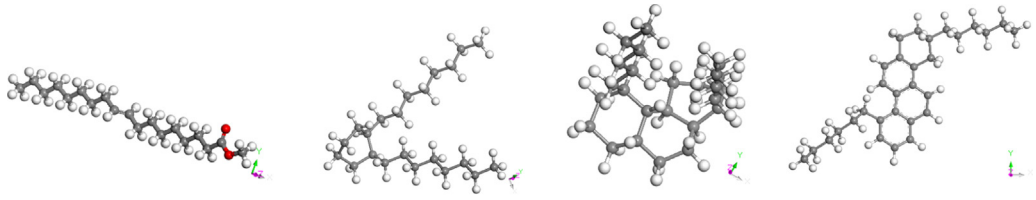

Fig. 3. The average molecular structures of different rejuvenators. (Grey: carbon atoms; White: hydrogen atoms; Red: oxygen atoms).

i. The initial bitumen and rejuvenator models with the lowest energy and stable configurations are subjected to the equilibrium dynamics procedure with an isothermal-isobaric ensemble (NPT, constant atomic number, simulation pressure, and temperature). The 1 fs (fs) and 200 picoseconds (ps) are set as the time step and total NPT simulation time. In addition, the Nose thermostat and Andersen barostat controlled the temperature of 298 K and pressure of 0.0001 GPa during the simulation. Moreover, the Ewald with the accuracy of 0.001 kcal/mol and Atom-based with the cutoff distance of 15.5 Å are assigned as the Electrostatic and van der Waals summation method.
ii. It should be noted that the bitumen and rejuvenator models will shrink into a stable and condensed state under external temperature and pressure conditions. However, the simulation time is insufficient for each molecule to relax and reach a thermodynamically stable point completely. Thus, the last configurations of bitumen and rejuvenator models in the NPT process are further implemented with an additional equilibrium dynamics procedure with a canonical ensemble (NVT, constant molecular number, model volume, and temperature). The temperature value, thermostat type, time step, and total simulation duration in the NVT process are consistent with the previous NPT step. Fig. 4 illustrates the final equilibrium molecular models of virgin and aged bitumen, as well as four rejuvenators, which are used for further performance prediction and analysis in terms of thermodynamics parameters, structural characteristics, and dynamic behaviors.

4.4. Validation of MD simulation outputs

The 25℃ density values of bitumen and rejuvenator models are measured through a pycnometer. Table 4 compares the density (ρ) values predicted from MD simulations with the experimental results. It can be found that the predicted ρ values of virgin and aged bitumen, as well as four rejuvenators, are close to the measured ones, which verifies the reasonability of bitumen and rejuve-

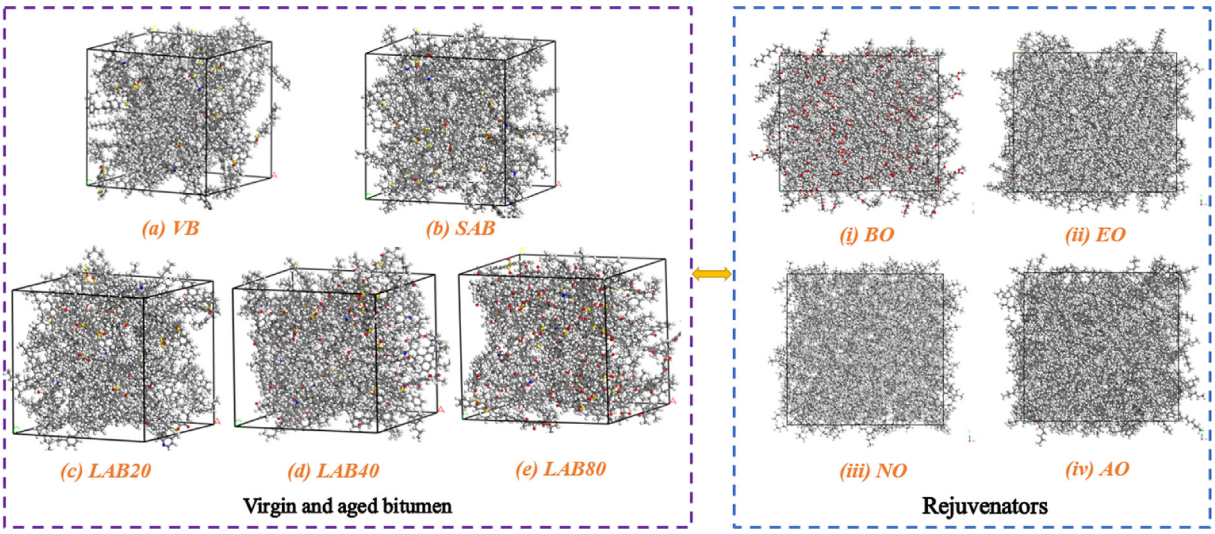

Fig. 4. Molecular models of the virgin, aged bitumen, and rejuvenators.

Table 4
The comparison of density values of bitumen and rejuvenators from MD simulations and experimental tests.

Bitumen samples	VB	SAB	LAB20	LAB40	LAB80
Predicted ρ ($g{\cdot}cm^{-3}$)	0.999	1.002	1.014	1.041	1.075
Measured ρ ($g{\cdot}cm^{-3}$)	1.017	1.019	1.024	1.036	1.054
Rejuvenators	BO	EO	NO	AO	–
Predicted ρ ($g{\cdot}cm^{-3}$)	0.886	0.821	0.868	0.971	–
Measured ρ ($g{\cdot}cm^{-3}$)	0.911	0.833	0.875	0.994	–

nator models together with MD simulation settings. The aged bitumen exhibits a larger density than virgin bitumen, which tends to be higher as the aging degree deepens. It is related to the increment of the asphaltene/maltene ratio and polar functional groups in aged bitumen, which distinctly enlarges the molecular weight and intermolecular force per volume unit [50]. Moreover, the density values of all rejuvenators are smaller than virgin and aged bitumen, which ensures their rejuvenation functions on density restoration of aged bitumen to virgin binder level. The density order for four rejuvenators from both MD simulations and experiments is the same as AO > BO > NO > EO. The high density of aromatic-oil and bio-oil is attributed to the polar aromatic structure and oxygen-containing ester function group, which significantly enhances the intermolecular interaction and tightness. However, there is still a slight difference in density parameter between MD simulation outputs and experimental results, which is due to the fact that the average molecular models of bitumen and rejuvenators utilized in this study incompletely match the realistic and detailed molecular components more than thousands of types in bitumen and 50 sorts in rejuvenators. Therefore, the averaging processing, as a simple way, may not consider the molecules with small and large molecular weights when the average molecular models of bitumen and rejuvenators are determined.

5. MD simulation results and discussion

5.1. Thermodynamics properties of aged bitumen and rejuvenators

From the viewpoint of composite material, the solubility parameter is an essential indicator to evaluate the compatibility between various components [56]. Furthermore, a well-known principle is that two materials with similar solubility parameter values would behave with greater compatibility [57]. Therefore, the compatibility potential between rejuvenators and aged binders is first evaluated through their solubility parameter (δ), which is strongly related to the cohesive energy density (CED). Both the CED and δ values of bitumen and rejuvenators can be predicted from MD simulations, as shown in Eqs. 1 and 2.

$$CED = \frac{E_{coh}}{V} = \frac{E_{vdw} + E_{ele}}{V} \quad (1)$$

$$\delta = \sqrt{CED} = \sqrt{\delta_{vdw}^2 + \delta_{ele}^2} \quad (2)$$

where CED and δ are the total cohesive energy density ($J{\cdot}cm^{-3}$) and solubility parameter ($(J{\cdot}cm^{-3})^{0.5}$), respectively; E_{coh} and V are the total cohesive energy and volume of simulation models; E_{vdw} and E_{ele} are the van der Waals and electrostatic term cohesive energy; δ_{vdw} and δ_{ele} are the van der Waals and electrostatic solubility parameter.

The cohesive energy in a molecular model comes from the non-bond intermolecular force, mainly consisting of van der Waals and electrostatic terms. Hence, the CED and δ parameters present van der Waal terms and electrostatic values. Table 5 displays the CED and δ parameters of the virgin, aged bitumen, and rejuvenators in terms of total, van der Waals, and electrostatic terms, which can be directly calculated and outputted by MD simulations after obtaining the equilibrium models. With the increment in an aging degree, all CED and δ values of bitumen show an increasing trend. The involvement of polar functional groups in aged bitumen molecules would remarkably enhance the intermolecular force and cohesive energy. That's why the aged bitumen with a higher aging level would show a larger stiffness.

Table 5
Cohesive energy density and solubility parameters of aged bitumen and rejuvenators.

Samples	CED ($J \cdot cm^{-3}$)	CED_{vdw} ($J \cdot cm^{-3}$)	CED_{ele} ($J \cdot cm^{-3}$)	δ $(J \cdot cm^{-3})^{0.5}$	δ_{vdw} $(J \cdot cm^{-3})^{0.5}$	δ_{ele} $(J \cdot cm^{-3})^{0.5}$
VB	3.357E8	3.229E8	4.126E6	18.322	17.968	2.029
SAB	3.360E8	3.236E8	3.624E6	18.331	17.989	1.901
LAB20	3.425E8	3.266E8	6.989E6	18.507	18.072	2.642
LAB40	3.675E8	3.474E8	1.074E7	19.171	18.638	3.276
LAB80	3.804E8	3.486E8	2.231E7	19.504	18.670	4.723
BO	3.190E8	3.073E8	4.764E6	17.862	17.529	2.180
EO	2.711E8	2.643E8	2.750E5	16.465	16.258	0.524
NO	2.723E8	2.649E8	2.837E5	16.501	16.275	0.532
AO	3.406E8	3.289E8	3.064E6	18.455	18.137	1.749

The CED and δ values of all rejuvenators are much smaller than virgin and aged bitumen, which further verifies that it is feasible to rehabilitate the CED and δ parameters of aged bitumen to the virgin level using these rejuvenators. However, these rejuvenators exhibit different CED and δ values, indicating a difference in restoration capacity on aged bitumen between these rejuvenators. This finding agrees well with the previous conclusion that the rejuvenation efficiency of the rejuvenator is influenced by the rejuvenator type and chemical components [58]. The sequence of CED and δ parameters for four rejuvenators is the same as AO > BO > NO > EO. It means that the CED and δ values of aromatic-oil rejuvenator are the closest to virgin and aged bitumen, followed by bio-oil, but the naphthenic-oil and engine-oil rejuvenator show a large gap in CED and δ values with virgin and aged binders. On the other hand, for all bitumen and rejuvenators, the electrostatic CED and δ values are much lower than the van der Waals ones. It implies that their CED and δ values are mostly contributed by the van der Waals interactions rather than the electrostatic term.

5.2. Validation from elemental analysis

In this study, the solubility parameters of bitumen and rejuvenators are calculated based on experimental data of elemental analysis to validate the accuracy of predicted δ values from MD simulations. The element distributions of virgin bitumen, aged bitumen, and different rejuvenators were measured at room temperature, and the experimental results are shown in Table 6. The difference in elemental compositions between the bitumen models (AAA-1, AAK-1, and AAM-1) proposed by Li and Greenfield [49] and the bitumen used in this study (named VB) is also discussed herein. Overall, the elemental composition of the VB binder is similar to that of these Li and Greenfield's models. However, the N% and O% values are both slightly higher than their developed models, but the C% of the former is 1.54 %, 1.74 %, and 2.84 % lower than the AAA-1, AAK-1, and AAM-1 model, respectively. In addition, the H % (10.90 %) of the VB is closest to the AAM-1 model, while its S% value (3.52 %) is mostly approaching the AAA-1 and AAK-1 models (3.60 %).

Compared with virgin bitumen, the aged binders exhibit a smaller carbon and hydrogen dosage due to the increase of oxygen content during the aging oxidation process, which tends to be more severe as the aging level increases. Meanwhile, the aging degree shows no influence on the concentration of nitrogen and sulfur elements. Concerning the elemental compositions of rejuvenators, the bio-oil displays an apparent characteristic of high oxygen dosage, which is reflected by the ester group in its average molecular structure. Besides, the elemental compositions in the other three petroleum-based rejuvenators are mainly composed of carbon and hydrogen atoms, which present hydrocarbon characteristics [55]. Various rejuvenators exhibit different carbon and hydrogen elements distribution. The engine-oil shows the lowest C% and highest H% values, followed by the naphthenic-oil rejuvenator, while the aromatic-oil has the opposite characteristic of the largest C% and smallest H% values.

The solubility parameter (δ) values of rejuvenators and bitumen can be calculated using an empirical formula, which was developed on heavy oils based on the relationship between the δ value and elemental compositions. Previous studies revealed that the correlation equation is efficient in predicting the δ values of petroleum distillates, which are similar to the results from a solvent titration method [56,59,60]. In addition, the titration method is cumbersome and not environmentally friendly, with different chemical solvents involved. Eq. 3 lists the empirical formula connecting the δ parameter with elemental compositions.

$$\delta = \frac{7.0 + 63.5f_a + 63.5\frac{H}{C} + 106\frac{O}{C} + 51.8\frac{N+S}{C}}{-10.9 + 12f_a + 13.9\frac{H}{C} + 5.5\frac{O}{C} - 2.8\frac{N+S}{C}} \quad (3)$$

Table 6
The elemental compositions of bitumen and rejuvenators.

Bitumen	N%	C%	H%	S%	O%
VB	0.90	84.06	10.90	3.52	0.62
AAA-1*	0.40	85.60	10.00	3.60	0.40
AAK-1*	0.50	85.80	10.00	3.60	0.40
AAM-1*	0.70	86.90	11.00	1.40	0.40
SAB	0.91	83.72	10.86	3.51	1.00
LAB20	0.92	83.26	10.75	3.49	1.58
LAB40	0.90	83.02	10.44	3.53	2.11
LAB 80	0.91	82.14	10.10	3.54	3.31
Rejuvenators	N%	C%	H%	S%	O%
BO	0.15	76.47	11.96	0.06	11.36
EO	0.23	85.16	14.36	0.13	0.12
NO	0.12	86.24	13.62	0.10	0.10
AO	0.55	88.01	10.56	0.48	0.40

*AAA-1, AAK-1, and AAM-1 are the virgin bitumen models proposed by Li and Greenfield [49].

where H, C, O, N and S are the element concentrations in bitumen and rejuvenators, and f_a refers to the aromaticity, which is calculated as follows:

$$f_a = 1.132 - 0.560 * \left(\frac{H}{C}\right) \quad (4)$$

Table 7 lists the measured H/C ratio, fa, ρ, O%, and δ values of virgin and aged bitumen, as well as different rejuvenators. It suggests that the aging degree decreases the H/C ratio but shows an increasing influence on the fa, ρ, O%, and δ values of bitumen. The aromatic-oil has the lowest H/C ratio and highest fa, ρ, and δ values, while the engine-oil shows the largest H/C ratio and smallest fa, ρ, and δ parameters. In addition, the V_B indicator is the reference volume of the "average repeat unit" of bitumen samples proposed by Painter [60], which is calculated as follows:

$$V_B = \frac{V_m}{O} = \frac{1600}{O'd} \quad (5)$$

where O′ and d are the oxygen concentration and specific gravity of bitumen samples. It demonstrates that the V_B value of bitumen reduces gradually as the increase of aging degree.

The solubility parameter values of rejuvenators, virgin, and aged binders from both MD simulations prediction and experimental data calculation are presented side by side in Fig. 5 to assess the application potential of using MD simulations to predict the δ values of rejuvenators and aged binders, which is beneficial to preliminary judge their compatibility level without any laboratory test and design more efficient molecular structures of rejuvenators with excellent compatibility with aged bitumen. It is worth noting that the temperature would display a great influence on the δ values, and here only presents the result at 25℃. Fig. 5(a) demonstrates that the total δ values of all bitumen and rejuvenators predicted from MD simulations are close to the calculated values based on elemental analysis results. The finding is consistent with the previous density conclusion and further confirms the feasibility of MD simulations on bitumen and rejuvenator materials. Fig. 5(b) also displays the van der Waals and electrostatic δ values predicted from MD simulations. Although the van der Waals δ values are much larger than the electrostatic ones, the latter should be considered when the δ values of bitumen and rejuvenators are determined through MD simulations.

5.3. Solubility parameter difference Δδ

The solubility parameter difference Δδ values at 298 K between four rejuvenators (BO, EO, NO, AO) and aged binders with different aging degrees (LAB20, LAB40, LAB80) are calculated to assess their compatibility levels. The higher the Δδ value is, the worse the compatibility shows. The Δδ results from both MD simulations and experiments are shown in Fig. 6. It can be found that all Δδ values from both experiments and MD simulations are strongly dependent on the rejuvenator type and bitumen aging degree. When the aged bitumen is the same, the increasing sequence of total and van der Waals Δδ values for four rejuvenators is AO < BO < NO < EO, while the order of electrostatic Δδ values follows BO < AO < NO < EO. It suggests that the aromatic-oil rejuvenator exhibits the best compatibility potential with aged bitumen regardless of the bitumen aging levels, followed by the bio-oil and naphthenic-oil, while the engine-oil shows the worst compatible capacity with aged binders. It should be mentioned

Table 7
The structural parameters of aged bitumen and pure rejuvenators.

Samples	H/C	fa	ρ (g·cm^{-3})	O%	V_B	δ ((J·cm^{-3})$^{0.5}$)
VB	1.556	0.260	1.017	0.618	2546	18.340
SAB	1.556	0.261	1.019	1.004	1564	18.373
LAB20	1.549	0.265	1.024	1.582	988	18.456
LAB40	1.509	0.287	1.036	2.113	731	18.723
LAB80	1.475	0.306	1.054	3.312	458	19.016
BO	1.877	0.081	0.912	11.36	–	17.427
EO	2.023	0.001	0.833	0.120	–	16.083
NO	1.895	0.071	0.875	0.100	–	16.530
AO	1.440	0.326	0.994	0.400	–	18.779

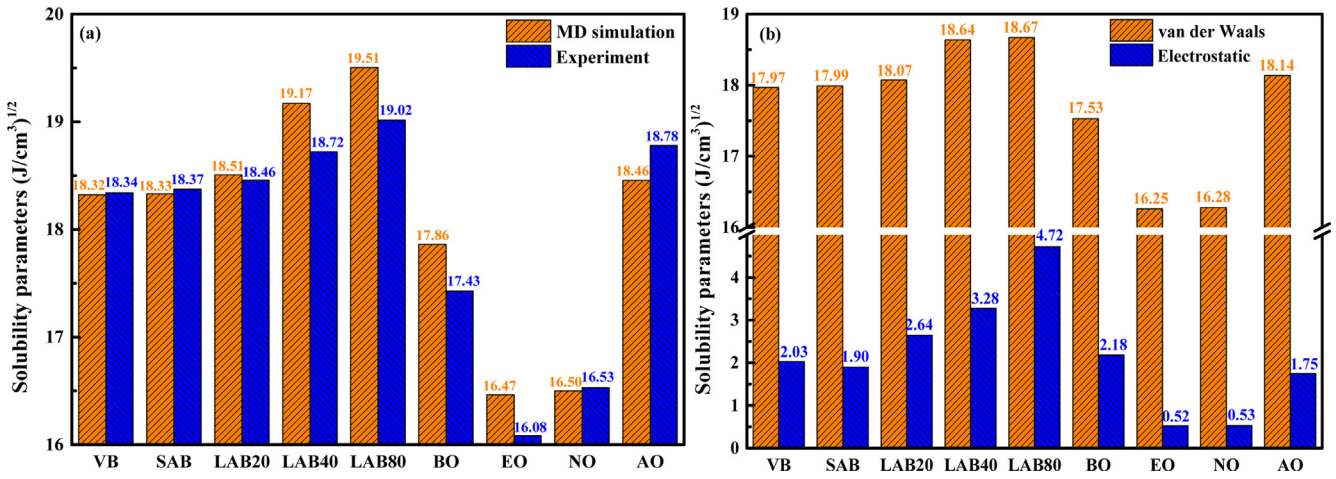

Fig. 5. The solubility parameter of virgin bitumen, aged bitumen, and rejuvenators (a) Total δ; (b) van der Waals and electrostatic δ.

that the conclusion from MD simulations output is consistent with the experimental result, which further verifies the efficiency of MD simulations on compatibility prediction of rejuvenators in aged bitumen.

On the other hand, with the aging degree of bitumen increases, the total, van der Waals, and electrostatic Δδ values from MD simulations and experiments all show an increasing trend. It was mentioned that the δ parameters of rejuvenators are lower than virgin and aged bitumen. The increment of the δ value for aged bitumen because of the deepening aging level would enlarge the difference in the δ parameter between the rejuvenator and aged bitumen. Meanwhile, the increased aging level would significantly enhance the intermolecular force of bitumen molecules, which leads to the elevated difficulty for rejuvenator molecules to break the strong interaction and be compatible with them. Thus, the compatibility potential between the rejuvenator and aged bitumen is weakened as the aging degree of bitumen increases. It is worth noting that the aromatic-oil rejuvenator still presents the much lower Δδ value and best compatibility with long-term aged bitumen for 80 h, which is least affected by the aging degree of bitumen. Interestingly, when the long-term aging duration of bitumen rises from 20 h to 80 h, the increment levels of Δδ values for bio-oil, engine-oil, and naphthenic-oil are similar. In addition, it is manifested that the total Δδ values between rejuvenators and aged binders are not the simple combination of van der Waals and electrostatic terms. The total Δδ values from both MD simulations and experiments are closer to the van der Waals Δδ than the electrostatic ones.

5.4. Flory-Huggins interaction parameter and mixing free energy

The Flory-Huggins theory is a classic principle for evaluating the compatibility of compatibility level and blending potential between various types of polymers and additives in composites [61]. Bituminous material behaves as a similar viscoelastic characteristic to polymers, and it is assumed that the Flory-Huggins theory can be adopted herein to assess the compatibility between rejuvenators and aged bitumen. Two crucial parameters, Flory-Huggins parameter χ and mixing free energy ΔG_m, are utilized and calculated as follows:

$$\chi = \frac{V_B}{RT}(\delta_B - \delta_R)^2 \tag{6}$$

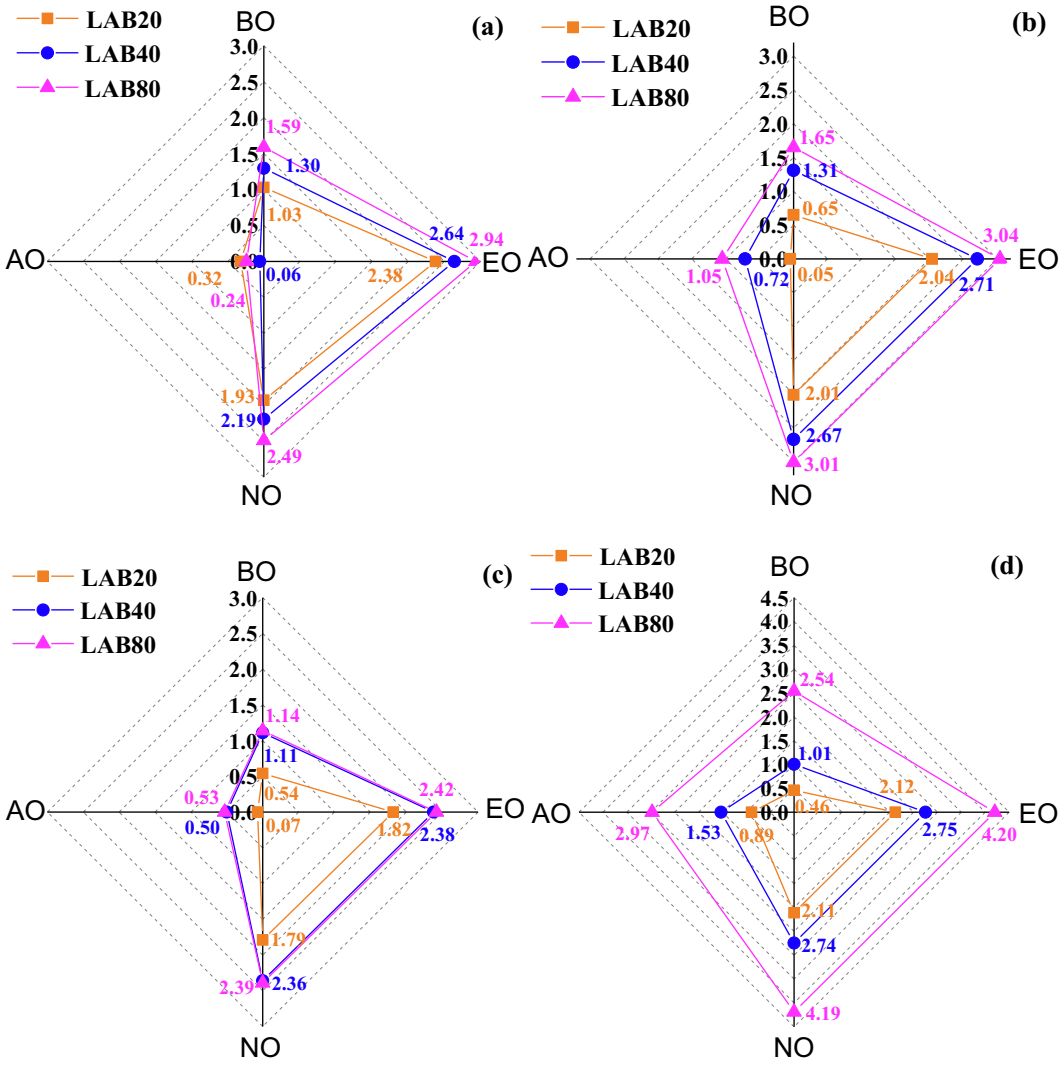

Fig. 6. The solubility parameter difference Δδ between rejuvenators and aged binders.

where χ is the Flory-Huggins interaction factor; δ_B and δ_R are the solubility parameter value of aged bitumen and rejuvenator; V_B refers to the reference volume of the "average repeat unit" of bitumen; T and R show the temperature (K) and gas constant (8.314 $J{\cdot}K^{-1}{\cdot}mol^{-1}$), respectively.

$$\frac{\Delta G_m}{RT} = \frac{\varnothing_R}{x_R}\ln\varnothing_A + \frac{\varnothing_B}{x_B}\ln\varnothing_B + \varnothing_R\varnothing_B\chi \quad (7)$$

where ΔG_m is the mixing free energy; $\varnothing_R$ and $\varnothing_B$ represent the volume fraction of rejuvenator and aged bitumen in rejuvenated binder; χ refers to the Flory-Huggins parameter.

From Eqs. 6 and 7, both χ and ΔG_m are dependent on the temperature T, indicating that the compatibility potential between rejuvenators and aged bitumen varies with temperature. Herein, the temperature is fixed at 25℃, and the temperature factor will be considered in the last section. Meanwhile, the mixing free energy ΔG_m is related to the volume fraction of the rejuvenator ($\varnothing_R$) and aged bitumen ($\varnothing_B$). The ΔG_m parameter represents the energy required when two materials are mixed completely. The negative ΔG_m values indicate that energy will be released from the mixing system to the environment, indicating that the mixing process is thermodynamically spontaneous. In this case, the larger the absolute value of ΔG_m is, the better the compatibility potential shows. However, the law will be the opposite when the ΔG_m value is positive. When the temperature and volume fraction is constant, the ΔG_m value is exclusively influenced by the Flory-Higgins parameter χ. Besides, a low χ value is beneficial to reducing the ΔG_m value and enhancing the compatibility extent between the rejuvenator and aged bitumen based on the correlation in Eq. 7.

According to Eq. 6, apart from the temperature and aged bitumen type, the Flory-Huggins parameter χ value is determined by the solubility parameter difference $\Delta\delta$ between the rejuvenator and aged bitumen. Overall, the more similar the δ values of rejuvenator and aged bitumen are, the lower the χ and ΔG_m values are, and the stronger the compatibility potential exhibits.

5.4.1. Flory-Huggins parameter χ

The Flory-Higgins interaction parameter χ values in various blending systems of rejuvenators and bitumen are calculated following Eq. 6. Herein, the solubility parameter δ values of rejuvenators, virgin, and aged bitumen from both experiments and MD simulations are utilized to show the difference in χ between measured and predicted values, which are listed in Table 8 and Table 9, respectively. Compared with the virgin and short-term aged bitumen, the χ values between bio-oil, engine-oil, and naphthenic-oil rejuvenators and long-term aged binders are higher. It implies that long-term aging weakens the compatibility level between these rejuvenators and bitumen. However, it is interesting to note that the χ values between the aromatic-oil rejuvenator and long-term aged bitumen are even lower than a virgin binder. The reason may be related to the enhanced intermolecular force through a Π-Π interaction. After long-term aging, more asphaltene molecules with polyaromatic structures are generated, which results in a stronger Π-Π interaction between the polyaromatic rings in asphaltene and aromatic-oil molecules [62].

Various rejuvenators show different χ values with the same aged bitumen. Regardless of the aged bitumen type, the χ values between the aromatic-oil rejuvenator and aged binders are the lowest, indicating that the aromatic-oil exhibits the best compatibility potential with aged binders. In contrast, the engine-oil rejuvenator shows higher χ values and the worst compatible capacity with aged binders. The χ values of bio-oil and naphthenic-oil systems are in the middle, and the former displays better compatibility with aged bitumen than the latter. Overall, the ranking of χ values for four rejuvenators from both experiments and MD simulations is the same as AO < BO < NO < EO. However, it should be mentioned that there is still little difference in χ values between experimental results and MD simulation outputs, mainly from the difference between established average structure and realistic multi-components characteristics of rejuvenators and aged binders. On the other hand, the aging degree of bitumen also affects the χ values and compatibility level between rejuvenators and aged bitumen, and its influence degree on various rejuvenators is different. From Eq. 6, the aging degree shows a complicated impact on χ values due to the variations of both V_B and $\Delta\delta$ parameters.

5.4.2. Mixing free energy ΔG_m

Tables 10 and 11 demonstrate the mixing free energy ΔG_{mix} values between rejuvenators and aged binders calculated with experimental data and MD simulation results. As mentioned above, the ΔG_{mix} value is affected by the Flory-Huggins interaction parameter (or solubility parameter difference) between rejuvenators and aged bitumen. It is also related to the temperature and volume fraction. This study aims to evaluate and compare the compatibility between different rejuvenators with aged binders. Thus, the temperature, volume fraction of the rejuvenator, and aged bitumen are fixed as 298 K, 0.1, and 0.9. It is found that all ΔG_{mix} values between various rejuvenators and aged binders are negative, indicating that the system energy is released when rejuvenators and aged binders are mixed. This mixing process is spontaneous, and a stable blend with lower energy can be obtained. However, when different rejuvenators are blended with aged bitumen at a fixed temperature and constant volume fraction, the ΔG_{mix} values are significantly different. The order of ΔG_{mix} val-

Table 8
Flory-Huggins parameters of different rejuvenated binders from experiments.

χ value	VB	SAB	LAB20	LAB40	LAB80	Ranking
BO	0.246	0.264	0.422	0.496	0.468	2
EO	1.503	1.547	2.246	2.056	1.590	4
NO	0.967	1.002	1.479	1.419	1.142	3
AO	0.057	0.049	0.042	0.001	0.010	1

Table 9
Flory-Huggins parameters of different rejuvenated binders from MD simulations.

χ value	VB	SAB	LAB20	LAB40	LAB80	Ranking
BO	0.063	0.065	0.168	0.506	0.502	2
EO	1.019	1.027	1.668	2.161	1.715	4
NO	0.979	0.987	1.609	2.102	1.673	3
AO	0.005	0.0046	0.001	0.151	0.206	1

Table 10
Mixing free energy of different rejuvenated binders from experiments.

ΔG_{mix} ($J \cdot mol^{-1}$)	T (K)	$\varnothing_R$	$\varnothing_B$	VB	SAB	LAB20	LAB40	LAB80	Ranking
BO	298	0.1	0.9	−0.326	−0.324	−0.304	−0.309	−0.310	2
EO	298	0.1	0.9	−0.210	−0.205	−0.152	−0.131	−0.204	4
NO	298	0.1	0.9	−0.260	−0.257	−0.216	−0.208	−0.247	3
AO	298	0.1	0.9	−0.325	−0.326	−0.334	−0.328	−0.337	1

Table 11
Mixing free energy of different rejuvenated binders from MD simulations.

ΔG_{mix} ($J \cdot mol^{-1}$)	T (K)	$\varnothing_R$	$\varnothing_B$	VB	SAB	LAB20	LAB40	LAB80	Ranking
BO	298	0.1	0.9	−0.351	−0.351	−0.313	−0.343	−0.320	2
EO	298	0.1	0.9	−0.261	−0.261	−0.141	−0.193	−0.193	4
NO	298	0.1	0.9	−0.254	−0.254	−0.144	−0.193	−0.191	3
AO	298	0.1	0.9	−0.331	−0.332	−0.326	−0.335	−0.328	1

ues for four rejuvenators is the same as that of the χ parameter. To all aged binders, the aromatic-oil rejuvenator shows the lowest ΔG_{mix} and the largest compatible capacity with aged bitumen. Compared to the naphthenic-oil, the bio-oil exhibits lower ΔG_{mix} values and better compatibility behavior, while the engine-oil presents the highest $\Delta G_{mix,}$ and there is a terrible compatibility issue between the engine-oil rejuvenator and aged bitumen. This conclusion is consistent with the findings in previous studies [63].

5.5. Intermolecular binding energy

The compatibility potential between rejuvenators and aged binders has been evaluated through different thermodynamics parameters of $\Delta\delta$, χ, and ΔG_{mix}. However, all of these parameters come from the independent bitumen and rejuvenator systems, and the compatibility mechanism from the viewpoint of intermolecular interaction is still unclear. Therefore, the molecular models of various rejuvenated bitumen composed of different rejuvenators and aged binders are established. The intermolecular energy between the rejuvenator and aged bitumen molecules is calculated to estimate their compatibility levels.

The model establishment and MD simulation procedures of all rejuvenated binders are the same as the aged bitumen and rejuvenators, which have been introduced in section 3.3. In rejuvenated bitumen models, rejuvenator molecules with 10 % atomic weight are mixed with aged bitumen molecules. The molecular numbers of various rejuvenators in different aged bitumen are listed in Table 12. To simplify, the short name of the rejuvenated binder model is composed of bitumen aging degree, rejuvenator dosage, and type. For instance, the rejuvenated bitumen composed of LAB20 aged bitumen and 10 % bio-oil rejuvenator is called "1P10B". It should be noted that the LAB20, LAB40, and LAB80 aged binders are also named 1P, 2P, and 4P, respectively. Fig. 7 illustrates the molecular equilibrium models of all rejuvenated binders with different rejuvenators and aged binders after the geometry optimization and MD simulation processes with NPT and NVT ensembles. This section focuses on the intermolecular energy between the rejuvenator and aged bitumen molecules. The following section will discuss the structural parameters regarding the molecular dispersion level.

(Grey: bitumen molecules; Yellow: bio-oil molecules; Orange: engine-oil molecules; Green: naphthenic-oil molecules; Brown: aromatic-oil molecules).

Generally, the energy of a hybrid system is lower than the sum of the energies of its constituent components, and the energy is released to keep it more thermodynamically stable when the hybrid system is framed. In this study, the binding energy $E_{binding}$ was utilized to assess the molecular interaction strength and compatibility level between the rejuvenator and aged bitumen molecules, which is calculated as follows:

$$E_{binding} = -E_{inter} = -(E_{total} - E_B - E_R) \quad (8)$$

where E_{total}, E_B, and E_R are the potential energy of the whole rejuvenated bitumen, aged bitumen phase, and rejuvenator phase, respectively.

The binding energy is a negative value of the interaction energy, representing the energy required to overcome the intermolecular force and separate the hybrid system into several independent phases. Therefore, the higher the binding energy value is, the stronger the intermolecular interaction between various molecules in different phases shows. Herein, the increased $E_{binding}$ suggests that the intermolecular interaction between the rejuvenator and aged bitumen molecules is enhanced, indicating greater compatibility between the rejuvenator and aged bitumen molecules.

Fig. 8 plots the binding energy $E_{binding}$ values between the rejuvenator and aged bitumen molecules in various rejuvenated bitumen models, which are calculated in terms of the potential energy, van der Waals energy, and electrostatic energy. It can be found that the electrostatic $E_{binding}$ values of all rejuvenated binders are much lower than the potential and van der Waals terms. Hence, it is concluded that the van der Waals interaction mainly contributes to the interaction force between the rejuvenator and aged bitumen molecules. Regardless of the aging level of bitumen, the potential, van der Waals, and electrostatic $E_{binding}$ values of aromatic-oil rejuvenated bitumen are the largest, followed by the bio-oil rejuvenated binder. In addition, the naphthenic-oil rejuvenated binders show higher $E_{binding}$ values than the engine-oil rejuvenated bitumen. It suggests that the intermolecular interaction between the aged bitumen and aromatic-oil molecules is the strongest, accelerating their blending degree. The reason may be that the polyaromatic structure in aromatic-oil rejuvenator could form the powerful Π-Π interaction with polar aromatic, resin, and asphaltene molecules retaining aromatic rings in aged bitumen.

Table 12
The molecular numbers of rejuvenators in different aged bitumen.

Aged bitumen	BO	EO	NO	AO
LAB20	13	13	10	9
LAB40	13	13	11	10
LAB80	14	13	11	10

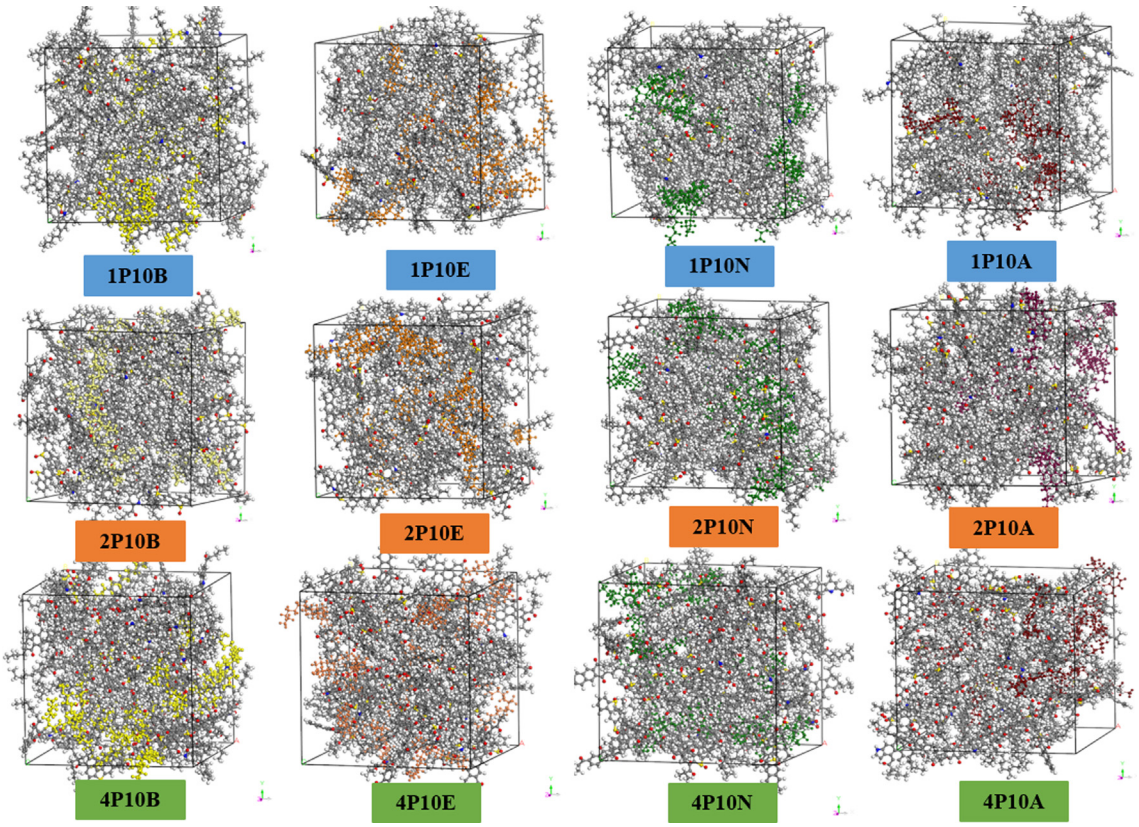

Fig. 7. Molecular models of various rejuvenated binders.

On the other hand, the intermolecular interaction of bio-oil and aged bitumen molecules are superior to the naphthenic-oil and engine-oil rejuvenators. It is related to the polar ester group in bio-oil molecular structure, which could form the hydrogen bond with aged bitumen molecules. From the viewpoint of intermolecular interaction strength, the compatibility potential ranking for these four rejuvenators is AO > BO > NO > EO, which is consistent with the previous conclusions from the thermodynamics parameters of $\Delta\delta$, χ, and ΔG_{mix}. At the same time, it is shown that the compatibility level between the aged bitumen and various rejuvenators can be predicted and compared through both thermodynamic parameters and intermolecular binding energy. It is beneficial to design a more efficient rejuvenator molecule with an excellent compatible capacity with aged bitumen in reclaimed asphalt pavement (RAP). The aging degree of bitumen also affects the binding energy $E_{binding}$ values with rejuvenators, but its influence level is lower than the molecular structure of rejuvenators. For both bio-oil and aromatic-oil rejuvenators, the $E_{binding}$ values reduce progressively as the bitumen aging becomes more serious, while the engine-oil rejuvenator shows the opposite trend.

5.6. Structural parameters in molecular models of rejuvenated binders

The dispersion level of polymers in aged bitumen is an important indicator in evaluating the compatibility between the polymers and the bitumen matrix. A high dispersion degree represents the better compatibility of polymer-modified bitumen. Herein, the dispersion degrees of rejuvenator molecules in rejuvenated bitumen models are estimated through the structural parameters of relative concentration (RC) and radial distribution function (RDF).

5.6.1. Concentration profile

The concentration profile computes the profile of atom density within evenly spaced slices. To run this calculation, a specific direction is divided into several bins, and the related atoms are counted. The relative concentration of a set of atoms in a slice is as follows:

$$RC_i = \frac{C_i}{C_{bulk}} = \frac{\left(\frac{N_i}{V_i}\right)}{C_{bulk}} \quad (9)$$

where RC_i means the relative concentration of the molecules in slice i.; C_i and C_{bulk} refer to the molecular concentration in slice i and the whole model, respectively; N_i is the number of particles in slice i, and V_i represents the volume of slice i.

Fig. 9 illustrates the relative concentration distribution of various rejuvenator molecules in LAB40 aged bitumen. Concerning a homogenous system, the relative concentration of molecules in all directions should be equal to 1.0. However, the relative concentration of rejuvenator molecules in rejuvenated bitumen fluctuates around 1.0. It implies that all rejuvenated bitumen models are heterogeneous at the molecular scale. Moreover, the relative concentration values of rejuvenator molecules in various directions differ significantly. The RC values are adopted to evaluate the molecular distribution levels of rejuvenator molecules. The molecular distribution tends to be more homogeneous when the whole RC distribution is closer to 1.0.

It is demonstrated that the molecular distribution behaviors of various rejuvenators are significantly different. The relative concentration distributions of engine-oil molecules in all directions are the most uniform and the closest to 1.0. On the contrary, the maximum value of the relative concentration of aromatic-oil molecules is>2.5, which is higher than the maximum points in relative concentration curves of bio-oil and naphthenic-oil mole-

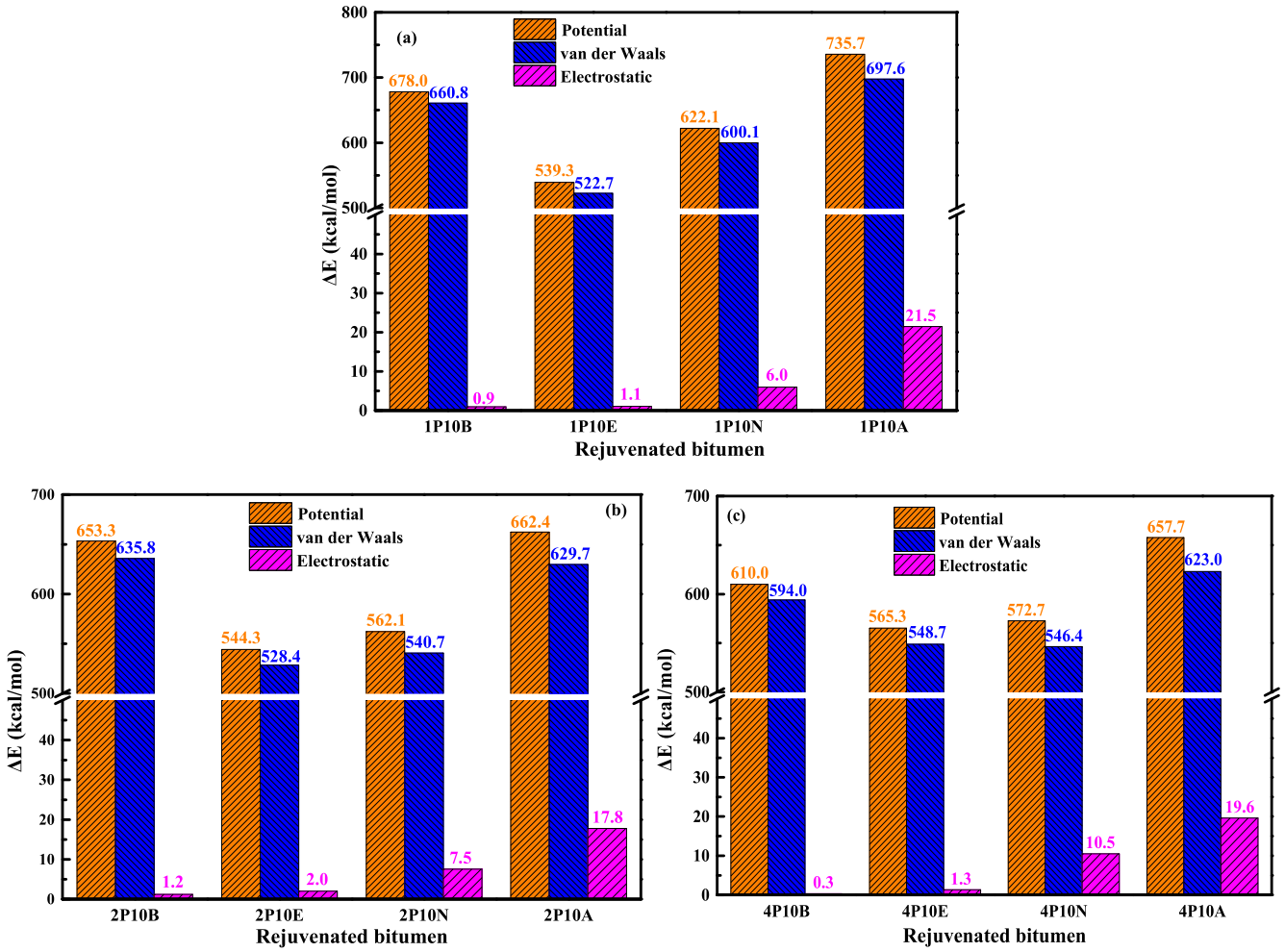

Fig. 8. The binding energy $E_{binding}$ values of various rejuvenated bitumen at 298 K(a) LAB20, (b) LAB40, (c) LAB80.

cules in their corresponding rejuvenated bitumen models. Therefore, the engine-oil rejuvenator shows the most homogeneous molecular distribution in rejuvenated bitumen, while the aromatic-oil rejuvenator exhibits the smallest molecular distribution level. The molecular distribution degree of bio-oil and naphthenic-oil molecules are in the middle, but the former presents a more uneven molecular distribution than the latter. The relative concentration profiles of these four rejuvenators in LAB20 and LAB80 aged bitumen are displayed in Figs. S1 and S2. The influence of bitumen aging degree on the relative concentration distribution of these rejuvenator molecules is limited. The ranking for molecular distribution level of four rejuvenators in LAB 20 aged bitumen is the same as that in LAB40 aged bitumen, which is EO > NO > BO > AO. However, the molecular distribution level of bio-oil molecules in LAB80 aged bitumen is more homogeneous than the other three rejuvenators.

5.6.2. Radial distribution function RDF

The intermolecular distance is another structural parameter to evaluate the molecular distribution of rejuvenator molecules in aged binders, which are outputted as follows:

$$g(r) = \frac{dN}{4\pi r^2 \rho dr} \quad (10)$$

where g(r) is the radial distribution function; N shows the molecular number in the whole rejuvenated bitumen model; ρ and r are the density ($g \cdot cm^{-3}$) and distance from the specified molecule (Å), respectively.

The RDF curves of different rejuvenator-rejuvenator molecular pairs in corresponding rejuvenated binders are demonstrated in Fig. 10. The rejuvenator molecules present similar RDF curves in aged binders with different aging degrees. However, there is a difference in g(r) and r values of RDF peaks between these four rejuvenators. The g(r) peak values of the engine-oil rejuvenator are lower than the other three rejuvenators, especially in LAB40 aged bitumen. It indicates that the intermolecular distance of engine-oil molecules is the smallest, which agrees well with the finding regarding its best molecular distribution level based on the relative concentration profile results. On the other hand, an additional g(r) peak at 1.4 Å for bio-oil and aromatic-oil molecules in their rejuvenated bitumen models. It implies that the intermolecular attraction potential of the BO-BO and AO-AO pair is more significant than the engine-oil and naphthenic-oil. The polar ester group in the bio-oil molecule and polyaromatic structure in the aromatic-oil molecule enlarge their intermolecular attraction force and reduce the molecular distribution degree. Moreover, the g(r) values at 1.4 Å of aromatic-oil molecules are remarkably higher than that of bio-oil rejuvenator.

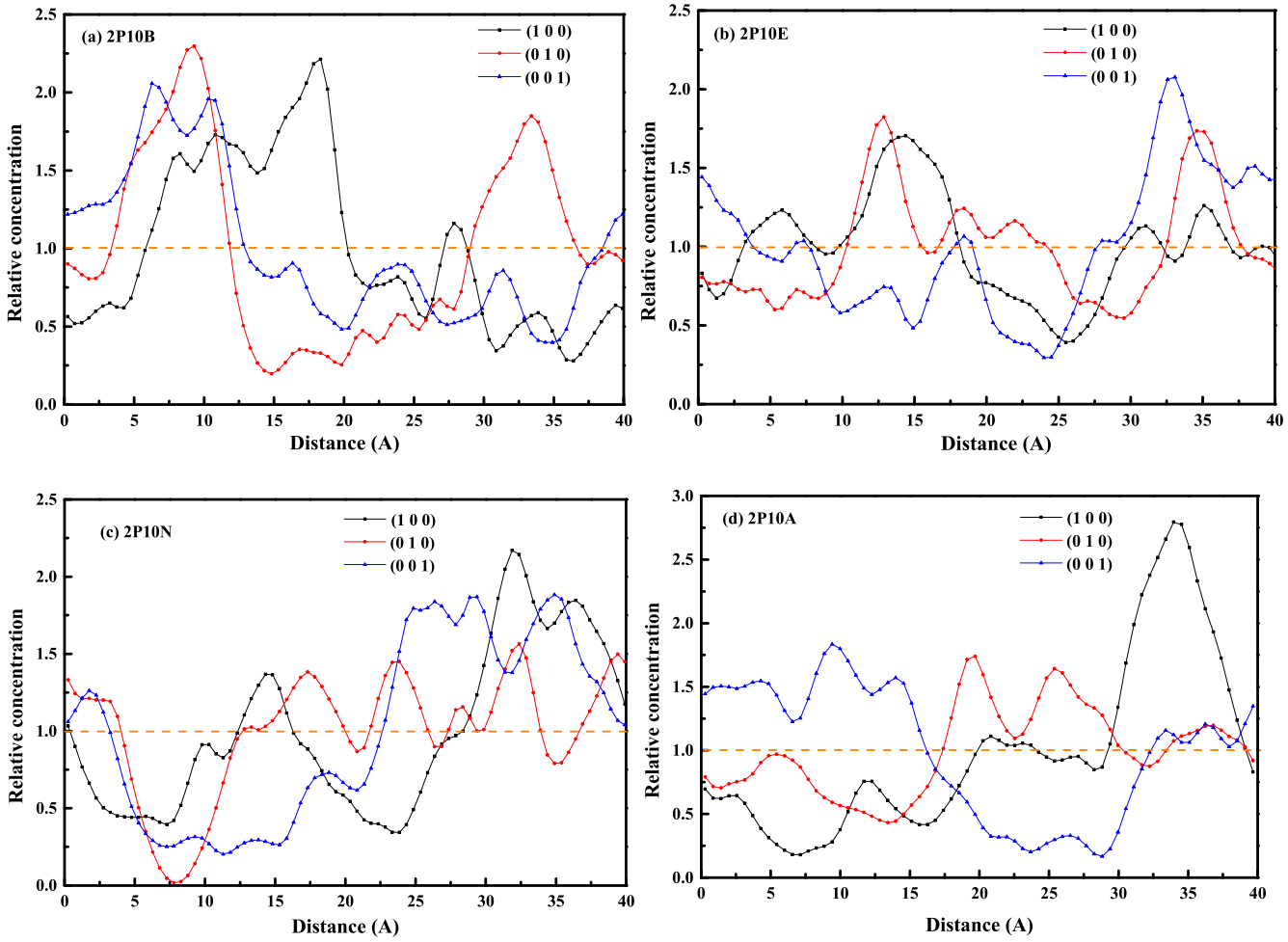

Fig. 9. The concentration distribution of rejuvenator molecules in rejuvenated binders with LAB40 aged bitumen.

In summary, the intermolecular attraction potential of aromatic-oil molecules is the largest, while its molecular distribution degree is the smallest. The engine-oil rejuvenator shows the lowest intermolecular attraction and the most homogeneous molecular distribution. Meanwhile, the intermolecular attraction and molecular distribution levels of the bio-oil and naphthenic-oil rejuvenators are in the middle, but the bio-oil rejuvenator displays a more heterogeneous molecular distribution and a larger intermolecular attraction potential than the naphthenic-oil rejuvenator.

The rejuvenated bitumen model is composed of rejuvenator and aged bitumen molecules, and it is of interest to explore the intermolecular distribution of various rejuvenators with the saturate, aromatic, resin, and asphaltene molecules in aged bitumen. Fig. 11 shows the RDF curves of rejuvenator-saturate, aromatic, resin, and asphaltene in different rejuvenated binders. The g(r) value is adopted to evaluate the intermolecular distribution level between two groups of molecules. A higher g(r) value represents the larger occurrence probability of rejuvenator molecules in SARA molecules of aged bitumen. It is found that the four kinds of rejuvenators exhibit variable occurrence probabilities with the SARA molecules. When the intermolecular distance between the rejuvenator and SARA molecules is fixed at 6 Å, the bio-oil molecules show a stronger interaction with the saturate, asphaltene, and resin molecules than the aromatic molecules. Moreover, the g(r) value of EO-Saturate is the highest, followed by the EO-Resin and EO-Aromatic pairs. In contrast, the EO-Asphaltene pair has the smallest g(r) parameter. The naphthenic-oil molecules are closer to the resin molecules than the saturate and aromatic ones, while there is the weakest interaction between the naphthenic-oil and asphaltene molecules. For the aromatic-oil rejuvenator, the g(r) ranking for AO-SARA pairs is AO-Asphaltene > AO-Resin > AO-Aromatic > AO-Saturate. Therefore, the aromatic-oil and bio-oil molecules exhibit a larger interaction potential with asphaltene molecules of aged bitumen than the naphthenic-oil and engine-oil rejuvenators. In addition, the engine-oil molecules display a high and low interaction probability with saturate and asphaltene molecules. Based on the colloidal structure of bitumen, it is highly possible for aromatic-oil and bio-oil to penetrate the asphaltene core, while the naphthenic-oil and engine-oil are mostly distributed in the aromatic/resin phase and saturate phase, respectively.

5.7. Dynamic properties

At the atomic scale, all rejuvenator and aged bitumen molecules are not fixed, which are in a dynamic equilibrium state controlled by both molecular kinetic energy and intermolecular energy. Therefore, the intermolecular compatibility between the rejuvenator and aged bitumen molecules is associated with their molecular mobility. In this study, the molecular mobility of rejuvenator and aged bitumen molecules in rejuvenated bitumen models is estimated with the dynamic parameters of mean square displacement

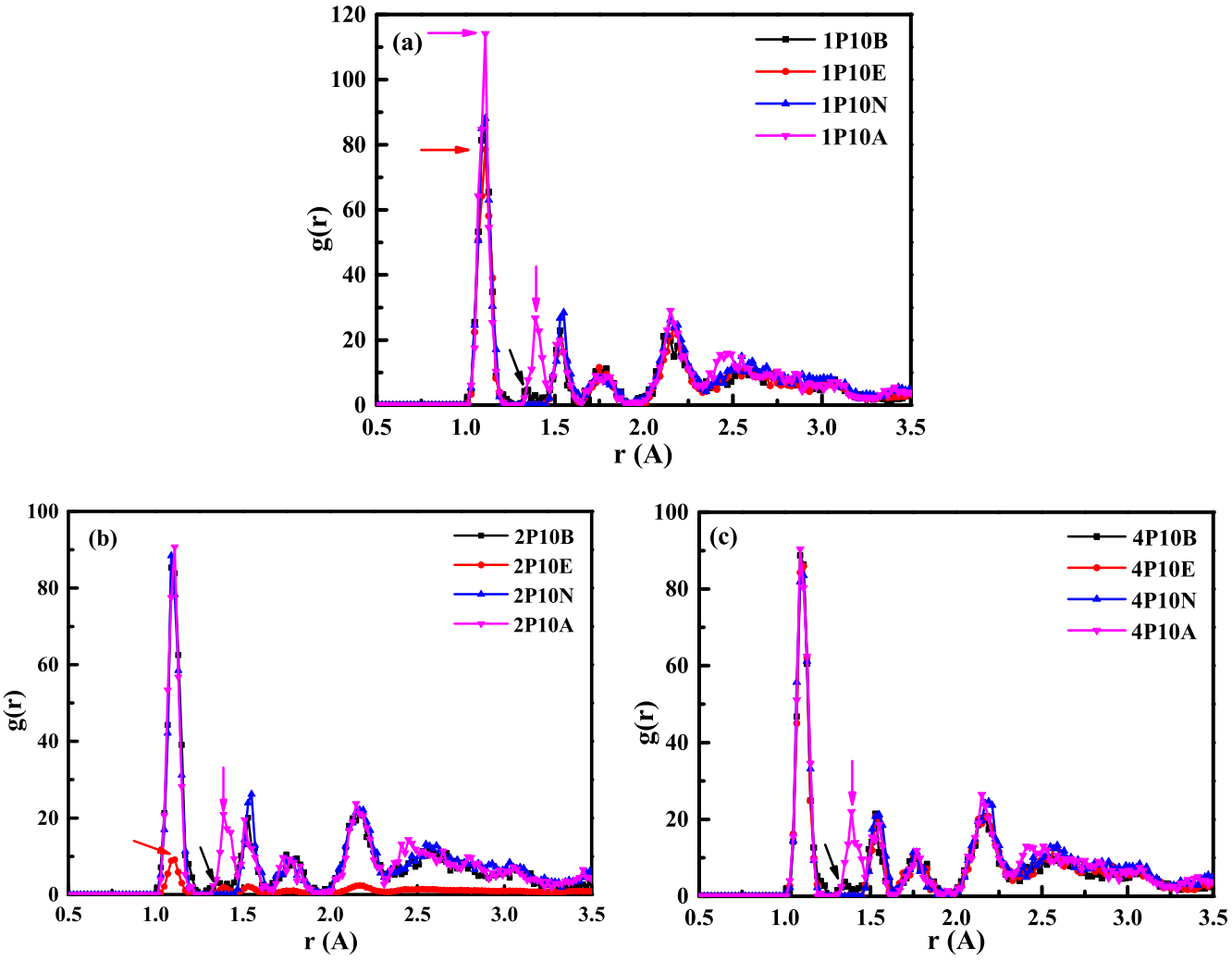

Fig. 10. RDF curves of rejuvenator-rejuvenator molecules in different rejuvenated bitumen with LAB40 aged bitumen.

(MSD) and diffusion coefficient (D), which are calculated and outputted from MD simulations following Eqs. 11 and 12.

$$MSD(t) = < \Delta r_i(t)^2 > = < [r_i(t) - r_i(0)]^2 > \quad (11)$$

$$D = \frac{1}{6N} \lim_{t \to \infty} \frac{d}{dt} \sum MSD(t) = \frac{a}{6} \quad (12)$$

where MSD refers to the mean square displacement of molecules at a simulation time t (ps); r_i (t) and r_i (0) are the molecular coordinates at the simulation time t and 0; D represents the diffusion coefficient, m^2/s; N is the total molecular number of molecules in a rejuvenated bitumen model, and a is the slope value in the correlation curve between the MSD parameter and simulation time.

Fig. 12 illustrates the MSD parameters of rejuvenator, saturate, aromatic, resin, and asphaltene molecules in various rejuvenated bitumen models versus the simulation time. Here only lists the MSD results of rejuvenated bitumen with LAB40 aged bitumen, and the corresponding results of the rejuvenated binders with LAB20 and LAB80 aged bitumen can be found in Supplementary Materials. The MSD values present an increasing trend as the simulation time prolongs due to the molecular movement during the MD simulations. When the simulation time keeps constant, the MSD values of SARA fractions in rejuvenated binders differ significantly. In all rejuvenated bitumen models, the saturate molecules exhibit larger MSD values than the aromatic and resin molecules, while the asphaltene molecules have the lowest MSD. It agrees well with the finding from previous studies that the saturate and asphaltene molecules show the highest and smallest molecular mobility in the bitumen model. The MSD parameters of aromatic and resin molecules are in the middle, and the former is larger than the latter.

On the other hand, the MSD values of rejuvenator molecules in the corresponding rejuvenated bitumen models are significantly different. At the same simulation time, the MSD parameters of bio-oil molecules are the largest, followed by the engine-oil and naphthenic-oil, while the aromatic-oil molecules display the lowest MSD value. It implies that the sequence of molecular mobility for four rejuvenators is BO > EO > NO > AO. The bio-oil and engine-oil rejuvenators exhibit a much stronger molecular motion than the naphthenic-oil and aromatic-oil rejuvenators. The high molecular mobility of rejuvenator molecules promotes their homogeneous distribution in rejuvenated bitumen. It thus increases the potential of phase separation if their intermolecular interaction with aged bitumen molecules is insufficient under thermal conditions.

The diffusion coefficient D values of rejuvenator molecules in rejuvenated bitumen models are calculated following Eq. 12, and the results at 298 K are summarized in Table 13. The order of magnitude for D values of all rejuvenators is the same, regardless of the

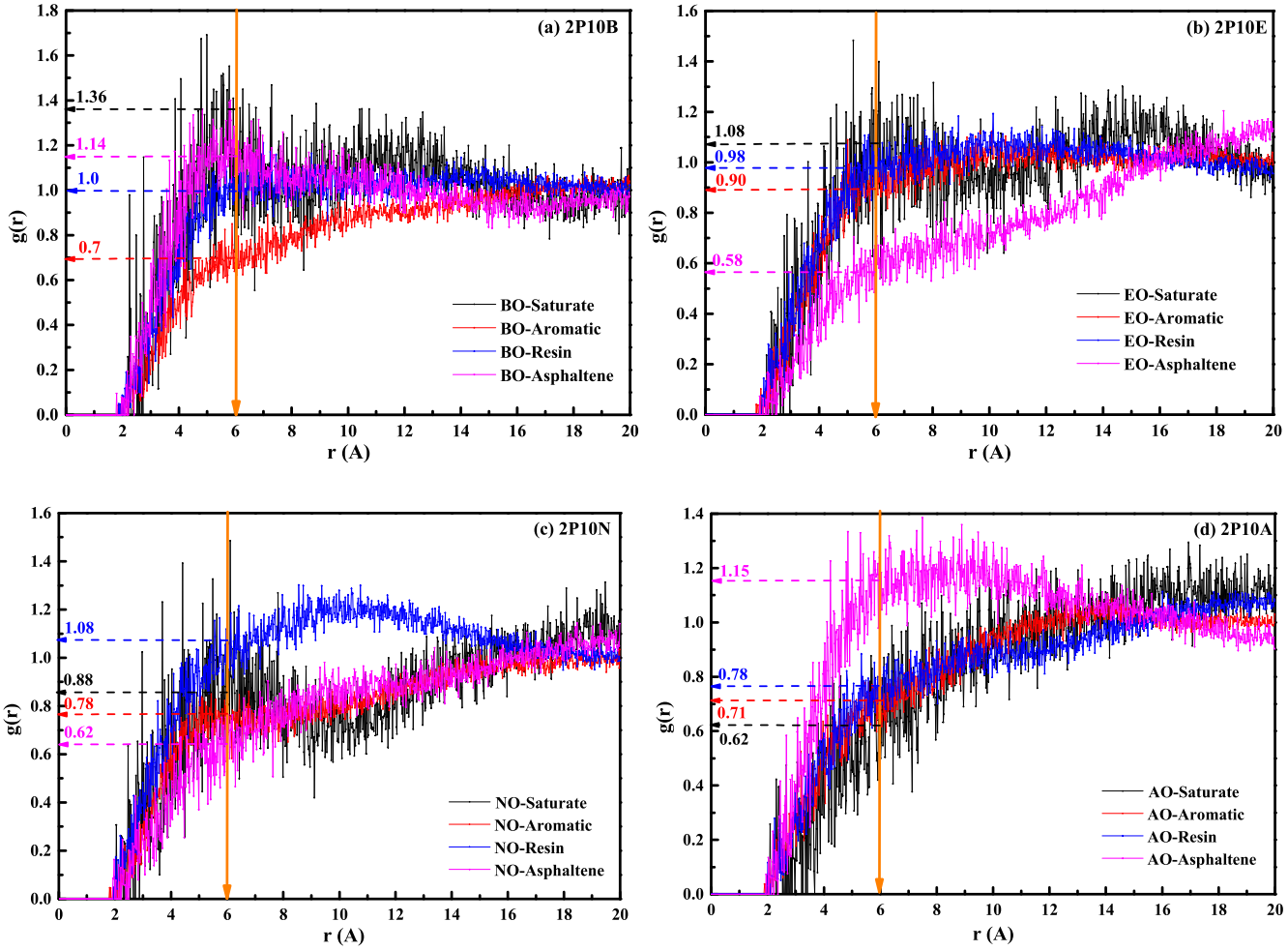

Fig. 11. RDF curves of rejuvenator-bitumen molecules in different rejuvenated bitumen with LAB40 aged bitumen.

rejuvenator type and aging degree of bitumen. However, there is a significant difference in D values between these four rejuvenators. When the aging degree of bitumen is the same, the bio-oil and aromatic-oil rejuvenator present the highest and lowest D values. Meanwhile, the D parameters of engine-oil and naphthenic-oil are in the middle, and the former has a higher value than the latter. In detail, the bio-oil molecules display 2.17, 1.71, and 4.35 times higher D values than the aromatic-oil in rejuvenated binders with the aged bitumen LAB20, LAB40, and LAB80, respectively. With the increase of bitumen aging degree, the diffusion coefficient values of all rejuvenators decrease gradually. Compared to the LAB20, the D values of bio-oil, engine-oil, naphthenic-oil, and aromatic-oil molecules in LAB80 aged bitumen reduce by 41.60 %, 61.82 %, 56.25 %, and 70.85 %, respectively. Thus, the aging level of bitumen has the greatest and smallest influence on the diffusive capacity of aromatic-oil and bio-oil molecules in rejuvenated binders.

6. Experimental results and discussion

In this study, the compatibility levels between various rejuvenators and aged binders with different aging degrees are investigated and validated through the thermal storage stability test, which is the most general method for compatibility evaluation of polymer-modified bitumen [44] and bio-bitumen [64]. After a thermal storage process, both DSR and FTIR tests are performed to evaluate the homogenous degrees of rheological and chemical parameters between different sections of rejuvenated bitumen samples after a thermal storage procedure. The rheological indices of complex modulus G*, phase angle δ, rutting factor G*/sinδ, and fatigue factor G*sinδ from the frequency sweep tests, the zero-shear viscosity ZSV from the flow tests, and the recovery percentage R% and non-recoverable creep compliance Jnr values from the MSCR tests, of the bottom, middle, and top sections in each rejuvenated bitumen are measured. Meanwhile, the carbonyl index C=O and sulfoxide index S=O of these specimens are obtained from the FTIR curves. To assess the thermal storage stability of different rejuvenated binders, an efficient parameter of separation index SI based on various rheological and chemical properties is calculated as follows:

$$SI = \frac{P_{max} - P_{min}}{P_{ave}} * 100\% \quad (13)$$

where SI shows the separation index (%); P represents one of the rheological and chemical parameters; P_{max}, P_{min}, and P_{ave} are the maximum, minimum, and average values of parameter P among the bottom, middle, and top sections of each rejuvenated bitumen after the thermal storage process. Hence, the lower the SI value is, the better the thermal phase stability of rejuvenated bitumen is shown.

6.1. Separation index based on G*, δ, G*/sinδ, and G*sinδ

The frequency sweep tests output the rheological parameters of G*, δ, G*/sinδ, and G*sinδ of the bottom, middle, and top sections of

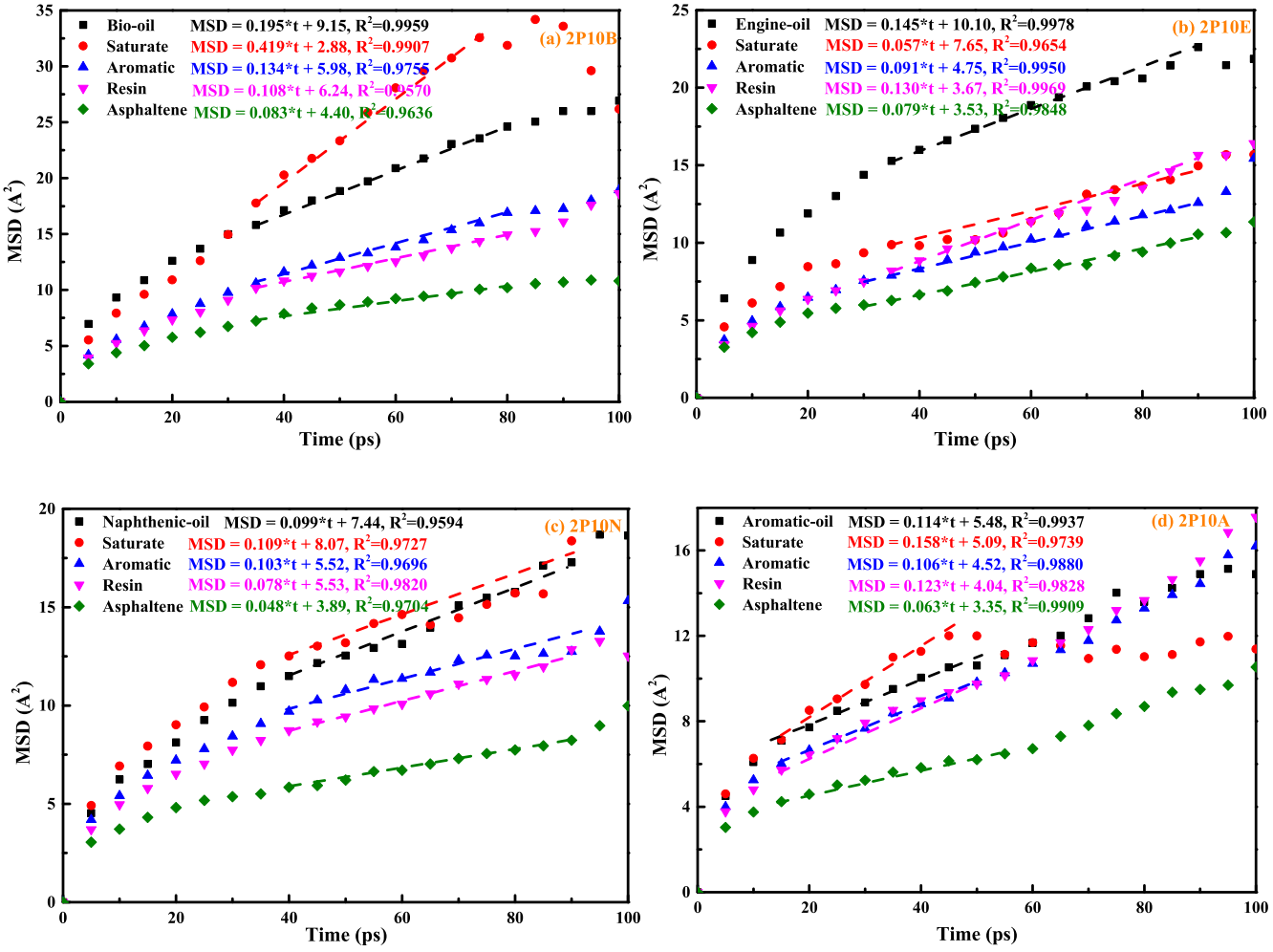

Fig. 12. The MSD values of rejuvenator and aged bitumen molecules versus the simulation time in different rejuvenated binders with LAB40 aged bitumen.

Table 13
The diffusion coefficient D of rejuvenator molecules in different rejuvenated binders.

D (m^2/s)	BO	EO	NO	AO
LAB20	$5.36*10^{-10}$	$4.40*10^{-10}$	$3.20*10^{-10}$	$2.47*10^{-10}$
LAB40	$3.25*10^{-10}$	$2.42*10^{-10}$	$1.65*10^{-10}$	$1.90*10^{-10}$
LAB80	$3.13*10^{-10}$	$1.68*10^{-10}$	$1.40*10^{-10}$	$0.72*10^{-10}$

rejuvenated binders. Fig. 13 illustrates these rheological indices of 2P10B, 2P10E, 2P10N, and 2P10A rejuvenated binders at 30℃. With the same rejuvenator dosage of 10 wt%, the bio-oil rejuvenated bitumen exhibits the lowest G*, G*/sinδ, and G*sinδ, followed by the engine-oil and naphthenic-oil rejuvenated binders. The aromatic-oil rejuvenated bitumen has the largest G*, G*/sinδ, and G*sinδ. It implies that the ranking for these four rejuvenators regarding the restoration level on stiffness, rutting, and fatigue resistance of aged bitumen is BO > EO > NO > AO. In addition, the δ values of bio-oil and aromatic-oil rejuvenated bitumen are larger than the engine-oil and naphthenic-oil ones. Hence, the rejuvenation capacity of engine-oil and naphthenic-oil rejuvenators on the ratio of viscous and elastic performance of aged bitumen is limited.

Fig. 13 shows a difference in these rheological indices between the bottom, middle, and top sections of each rejuvenated bitumen after the thermal storage procedure. To directly assess and compare the thermal storage stability and compatibility between various rejuvenators and aged binders, the separation indices based on these rheological parameters are calculated following Eq. 13, and the corresponding results are displayed in Fig. 14. It should be mentioned that two temperatures of 30 and 60℃ are selected for all FS tests to ensure the reliability of conclusions.

The SI values of all rejuvenated binders depend on the rheological parameter type and testing temperature. For all kinds of rejuvenators, the SI values of rejuvenated binders with LAB40 and LAB80 aged bitumen measured at 60℃ are much larger than that at 30℃, while the rejuvenated binders with LAB20 aged bitumen show the opposite trend. In addition, the SI values based on the G*/sinδ and δ parameters of all rejuvenated binders are the highest and lowest, while SI parameters calculated from the G* and G*sinδ are similar regardless of the rejuvenator types, aging degree of bitumen, and testing temperatures. Thence, the G*/sinδ parameter is the most sensitive to evaluate the separation level of rejuvenated bitumen during the thermal storage process, while the δ parameter shows minimal sensitivity.

When the aging level of aged bitumen and testing temperature is fixed, the SI values based on all rheological indices of engine-oil rejuvenated bitumen are the highest, followed by the naphthenic-oil and bio-oil rejuvenated binders, while the aromatic-oil rejuvenated bitumen present the lowest SI values. The separation poten-

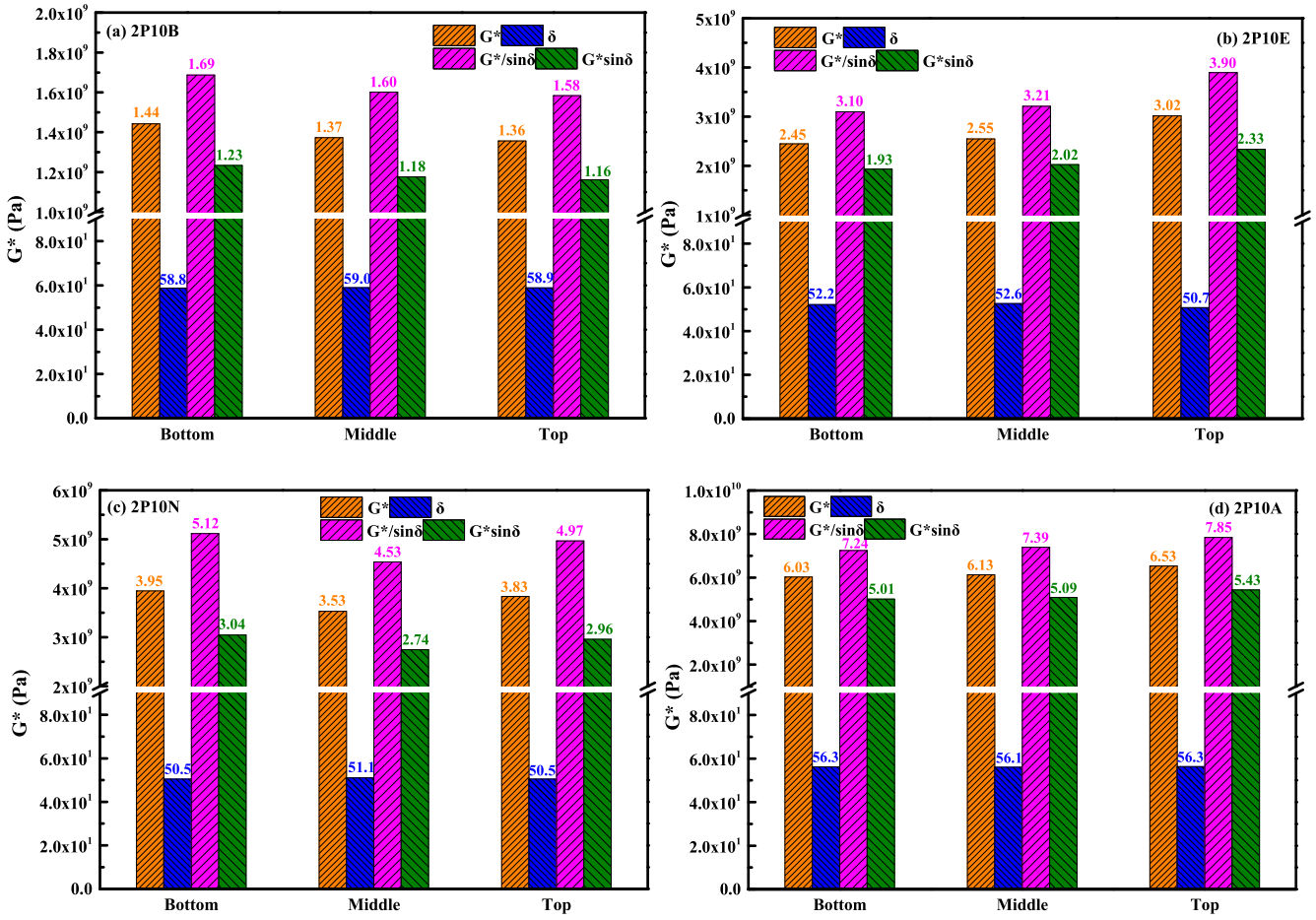

Fig. 13. The rheological parameters of the bottom, middle, and top sections in rejuvenated binders at 30℃.

tial of engine-oil in rejuvenated bitumen is the largest during the thermal storage process, while the aromatic-oil rejuvenated binder exhibits the most stable blending level. Meanwhile, the SI values of bio-oil and naphthenic-oil rejuvenated binders are in the middle, and the former is lower than the latter. It denotes that the order of separation potential for four rejuvenators is AO < BO < NO < EO, which is consistent with the compatibility sequence from both MD simulations and experiments. Therefore, the separation index parameters from the thermal storage test are strongly associated with the compatibility level between the rejuvenators and aged binders. The worst and best compatibility capacity of engine-oil and aromatic-oil rejuvenators contributes to their highest and lowest separation potential in rejuvenated binders during the thermal storage procedure. The separation index SI values of rejuvenated binders with the LAB20, LAB40, and LAB80 aged bitumen are significantly different, indicating that the separation potential of rejuvenators is also affected by the aging level of aged bitumen in rejuvenated binders. However, the influence of aging degree on the separation index values of various rejuvenated binders is not consistent, which agrees well with the previous conclusion regarding the role of aging degree on the compatibility between different rejuvenators and aged bitumen.

6.2. Separation index based on zero-shear viscosity

The steady-state flow tests are conducted to detect the difference in flow behaviors and zero-shear viscosity between the bottom, middle, and top sections of rejuvenated binders after a thermal storage stage. Fig. 15 illustrates the flow curves of three pieces in 2P10B, 2P10E, 2P10N, and 2P10A rejuvenated binders at 60℃. On the whole, the flow behaviors of all specimens are composed of the Newtonian flow region and shear-thinning range. It agrees well with the previous studies, which reported that the bituminous material exhibits the Newtonian flow characteristic, in which its viscosity values are independent of the shear rate. However, when the shear rate exceeds a crucial point, the viscosity values of bitumen reduce as the increment in shear rate dramatically, indicating a shear-thinning behavior. From Fig. 15, there is a difference in viscosity values and flow behaviors between the bottom, middle, and top sections of various rejuvenated binders after the thermal storage process.

The correlation curves between the shear rate and complex viscosity values of three sections in rejuvenated binders are fitted by the Carreau model:

$$\frac{\eta_0}{\eta} = \left[1 + \left(\frac{\gamma}{\gamma_c}\right)^2\right]^s \tag{14}$$

where η and γ are the complex viscosity (Pa·s) and shear rate (s^{-1}); η_0 represents the zero-shear viscosity, Pa·s; γ_c refers to the key shear rate related to the turning point before the shear-thinning region, s^{-1}, and s shows the slope value of the shear-thinning behavior range. It should be noted that the η_0 parameter is the critical viscosity when the shear rate reaches zero, which was proved to be an important indicator associated with the bitumen deformation resistance.

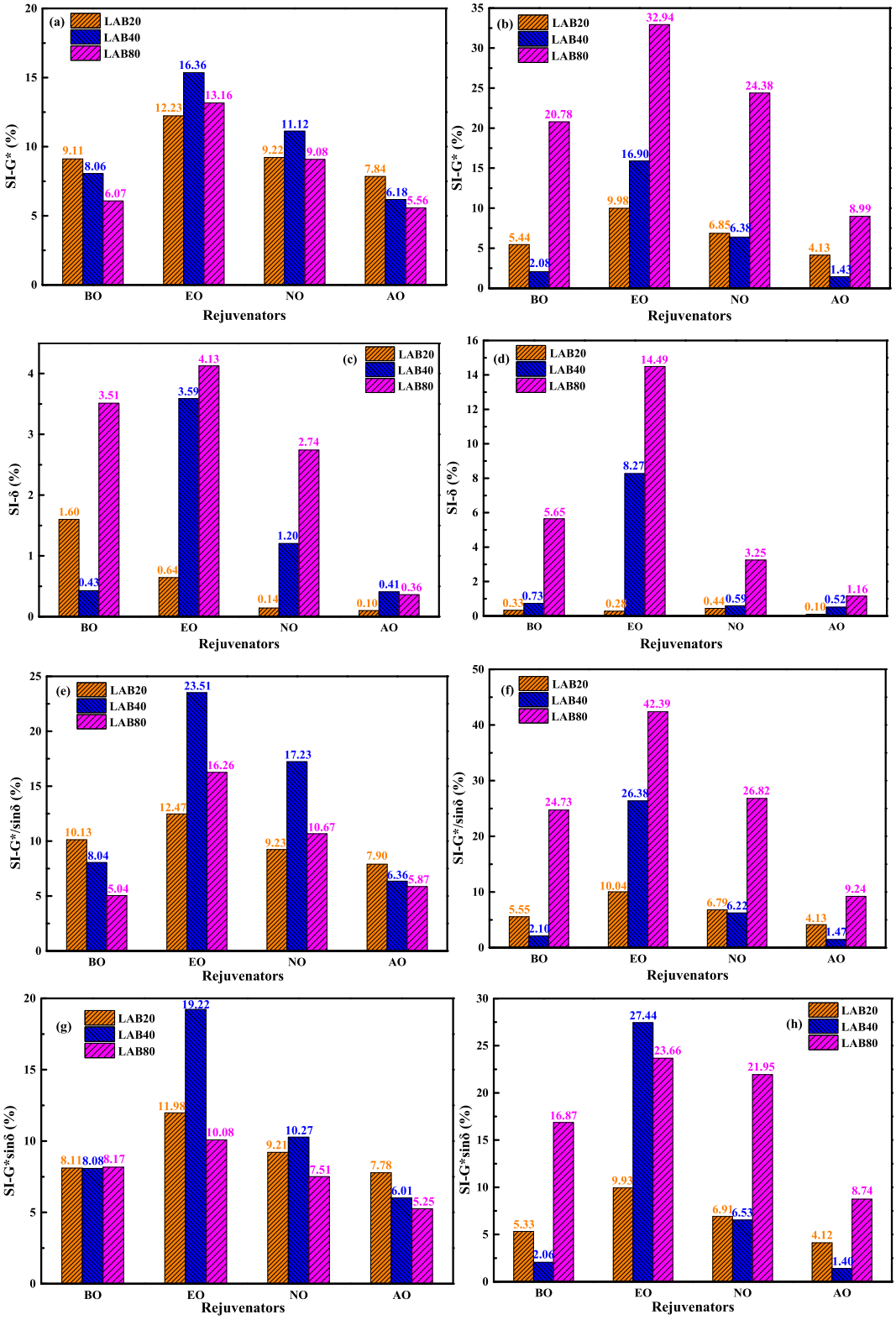

Fig. 14. The separation index SI values of rejuvenated binders based on G*(a)(b), δ (c)(d), G*/sinδ (e)(f), and G*sinδ (g)(h) at 30℃ and 60℃.

According to Eq. 14, the zero-shear viscosity (ZSV) of each section in rejuvenated binders can be outputted. The results are summarized in Fig. 16a-c considering the effects of rejuvenator type and aging degree of aged bitumen in rejuvenated bitumen. Overall, the ZSV values of rejuvenated binders with various rejuvenators are significantly different. Regardless of the aging level of bitumen, the bio-oil rejuvenated binders have the lowest ZSV values, followed by the engine-oil and naphthenic-oil rejuvenated binders, while the aromatic-oil rejuvenated bitumen shows the highest ZSV values. It implies that the ranking for these four rejuvenators on the restoration level of ZSV values of aged bitumen follows BO > EO > BO > AO. Furthermore, with the same rejuvenator dosage

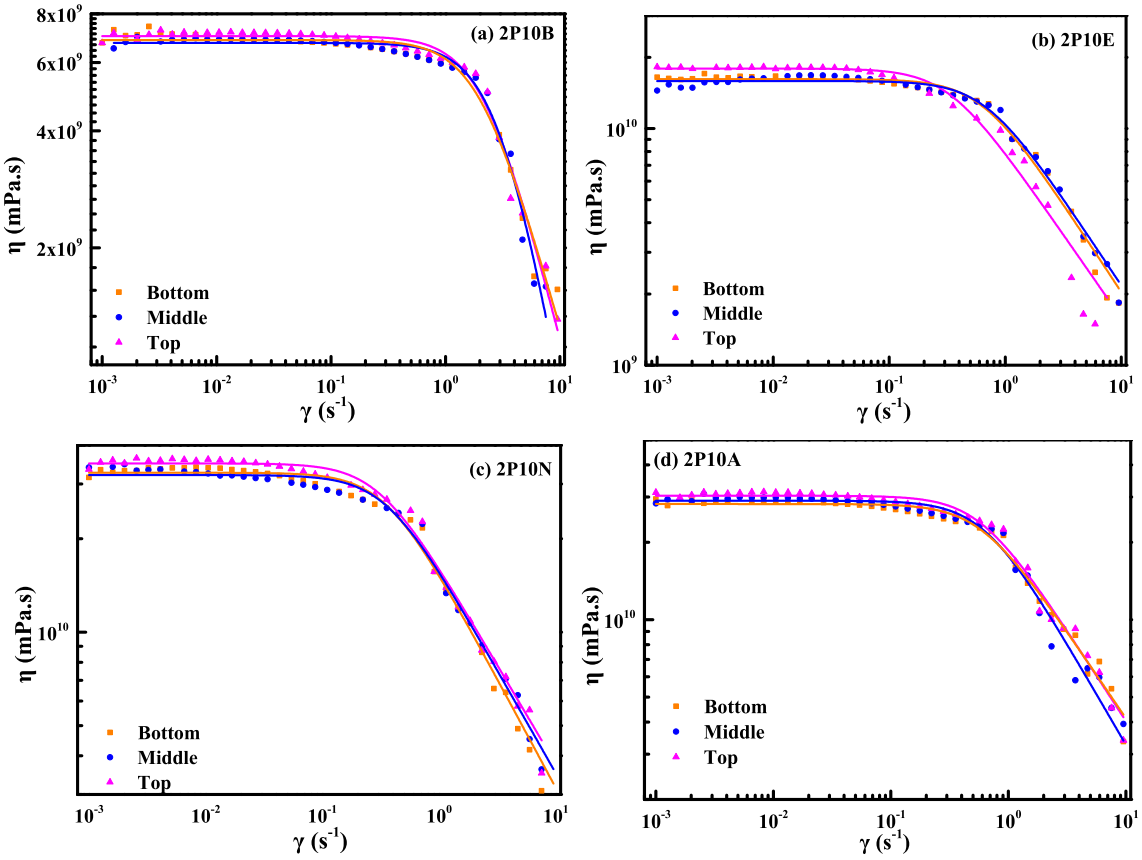

Fig. 15. Flow curves at 60℃ of the bottom, middle, and top samples in rejuvenated binders after the thermal storage.

and aging degree of bitumen, the aromatic-oil and naphthenic-oil rejuvenated binders exhibit stronger deformation resistance than the bio-oil and engine-oil rejuvenated bitumen.

Due to the constant rejuvenator dosage, the ZSV values of rejuvenated binders increase remarkably as the aging degree of bitumen deepens. It can be found that the thermal storage procedure leads to the difference in ZSV values between the bottom, middle, and top sections in rejuvenated bitumen. The separation index SI values based on the ZSV parameters of all rejuvenated binders are calculated using Eq. 13, and these SI values are shown in Fig. 16d. The SI values based on ZSV parameters of different rejuvenated binders also present the increasing law of AO < BO < NO < EO. It further validates that the aromatic-oil and bio-oil rejuvenators display better thermal phase stability and compatibility with aged bitumen than the naphthenic-oil and engine-oil. Moreover, the ZSV-based SI values of all rejuvenated binders are lower than that based on G*, G*/sinδ, and G*sinδ but higher than the δ-based ones. Interestingly, the role of the bitumen aging level in determining the separation potential of rejuvenators from aged bitumen can be evaluated according to the ZSV-based SI values. As the aging level of bitumen increases, the ZSV-based SI parameter of all rejuvenated binders increases gradually. It manifests that the thermal storage stability of rejuvenated binders with the same rejuvenator type and dosage shows a worse trend as the bitumen aging becomes more severe.

6.3. Separation index based on R% and Jnr

The multiple stress creep and recovery (MSCR) tests are performed on all rejuvenated binders after the thermal storage process at 52℃. The crucial parameters, recovery percentage R and non-recoverable creep compliance Jnr are measured at the stress of 0.1 kPa ($R_{0.1}$ and $Jnr_{0.1}$) and 3.2 kPa ($R_{3.2}$ and $Jnr_{3.2}$). Fig. 17 displays the MSCR parameters of the bottom, middle, and top sections in various rejuvenated binders with LAB40 aged bitumen.

From Fig. 17, the rejuvenated binders composed of aged bitumen and various rejuvenators exhibit different R% and Jnr values at both stress levels of 0.1 and 3.2 kPa. When the rejuvenator dosage is the same, the bio-oil rejuvenated bitumen presents the lowest $R_{0.1}$ and $R_{3.2}$ but the highest $Jnr_{0.1}$ and $Jnr_{3.2}$ values. However, the aromatic-oil rejuvenated binder has the largest R% and smallest Jnr values. The R% and Jnr values of engine-oil and naphthenic-oil rejuvenated binders are in the middle. Meanwhile, the naphthenic-oil rejuvenated bitumen shows higher R% and lower Jnr values than the engine-oil rejuvenated binder. In general, the aging of bitumen increases the R% but reduces the Jnr values, indicating that the aged bitumen owns a larger elastic component ratio and stronger deformation recovery capacity than the virgin bitumen. The rejuvenators are incorporated into aged bitumen to recover all chemical and rheological properties to the virgin bitumen level. The bio-oil rejuvenator displays the most prominent effects on restoring the R% and Jnr values of aged bitumen, while the aromatic-oil rejuvenator shows minimal recovery capacity. It further verifies that the rejuvenator efficiency on aged bitumen's rheological and mechanical performance strongly depends on the rejuvenator type and chemical components.

The separation index values based on MSCR parameters of the bottom, middle, and top sections in various rejuvenated binders are calculated and shown in Fig. 18. The SI values are dependent on the MSCR parameter selected, and the R%-based SI values are

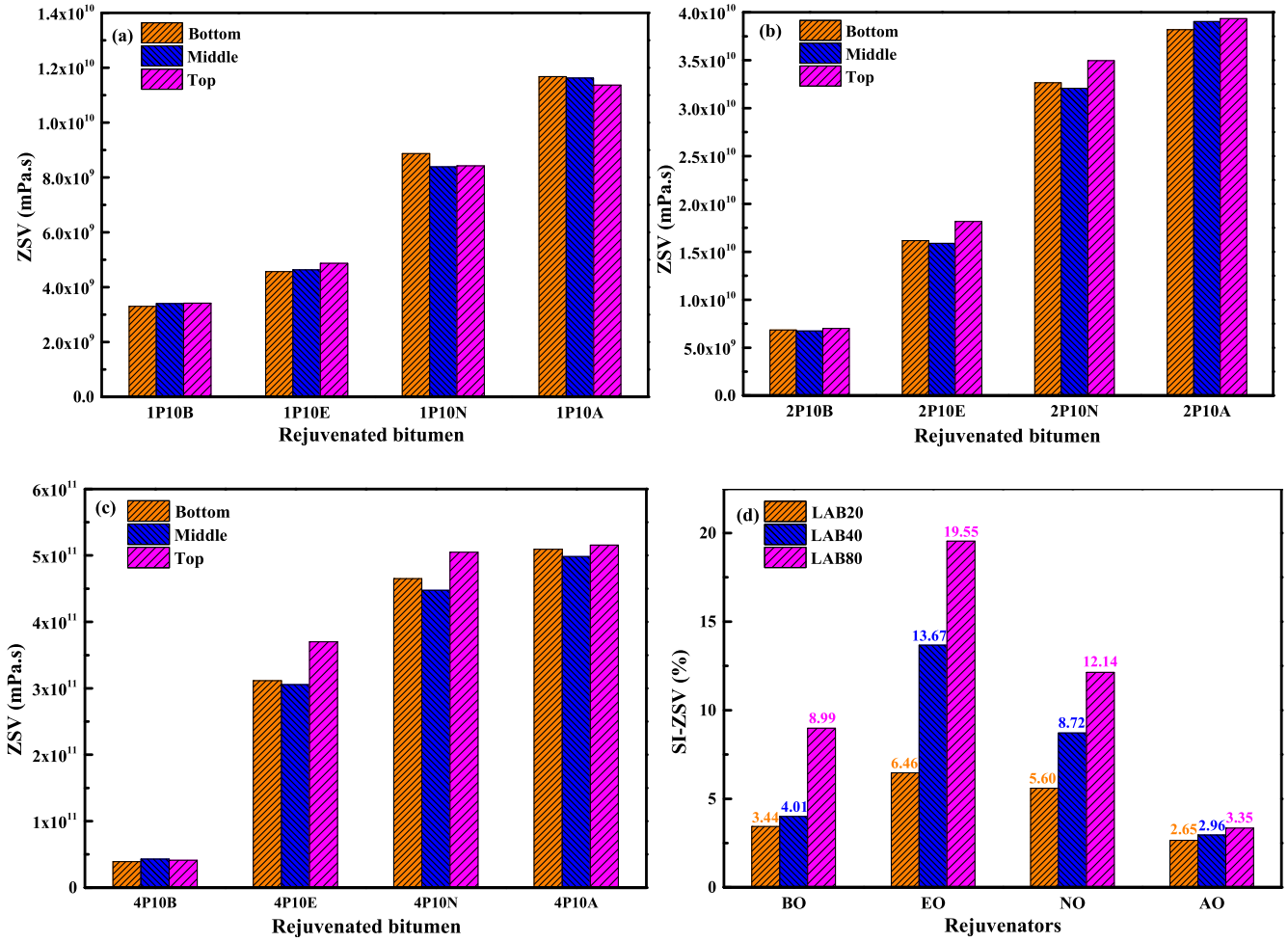

Fig. 16. Zero-shear viscosity and SI values of rejuvenated binders at 60℃ after a thermal storage process.

lower than Jnr-based SI. No matter which MSCR parameter is selected, the SI values of engine-oil rejuvenated binders are the largest, followed by the naphthenic-oil and bio-oil rejuvenated bitumen, while the aromatic-oil rejuvenated binders show the lowest SI values. The same conclusion is drawn that the sequence of SI values based on all rheological indices for four rejuvenators is AO < BO < NO < EO, which agrees well with the finding of their compatibility ranking from both MD simulations and experimental results. Therefore, the thermal storage test combined with rheological characterizations can be adopted to validate the compatibility behaviors of various rejuvenators in aged binders predicted from MD simulations. However, the SI values of rejuvenated binders are sensitive to the selected parameter type, and the unified rheological index should be used for all rejuvenated bitumen samples.

On the other hand, the thermal storage stability of rejuvenated bitumen is also influenced by the aging degree of bitumen. With the long-term aging level deepens, both R%-based and Jnr-based SI values of all rejuvenated binders show an increasing trend. For instance, the SI-$R_{3.2}$ values of BO, EO, NO, and AO rejuvenated binders increase by 3.22 %, 12.15 %, 6.16 %, and 0.51 %, while the SI-$Jnr_{3.2}$ values enlarge by 10.03 %, 33.78 %, 23.80 %, and 6.96 % when the aged bitumen varies from LAB20 to LAB80. Therefore, the thermal phase stability of engine-oil and naphthenic-oil rejuvenated binder are more sensitive to the aging degree variation of bitumen than the bio-oil and aromatic-oil rejuvenated bitumen.

6.4. Separation index based on chemical characteristics

Apart from the rheological indexes, the difference in chemical characteristics between different sections of rejuvenated binders is monitored through the FTIR test after thermal storage. Fig. 19 shows the FTIR curves of the bottom, middle, and top specimens in various rejuvenated bitumen.

In different rejuvenated binders, most of the characteristic peaks are the same when the aging level of bitumen keeps constant. The peaks at 2952 and 2862 cm^{-1} are related to the C—H stretch of methylene (—CH_2—) and methyl (—CH_3) in alkanes. Moreover, two characteristic peaks at 1460 and 1375 cm^{-1} come from a C—H bend of the —CH_2— and —CH_3 groups. It is worth noting that these common peaks in rejuvenated bitumen are both from the bitumen and rejuvenator molecules. In addition, there is still a difference in FTIR curves between different rejuvenated bitumen due to the difference in molecular structures of these rejuvenators. Compared to aged bitumen, there is no specific peak observed in engine-oil and naphthenic-oil rejuvenated binders, indicating that the chemical structures of engine-oil and naphthenic-oil are similar to the bitumen. However, two strong peaks at 1750 and 1160 cm^{-1} are detected in FTIR curves of bio-oil rejuvenated bitumen, which is related to the C═O and C—O—C stretch in the ester group. The peaks at 1030, 1600, and 1700 cm^{-1} are found in FTIR curves of all rejuvenated binders, which refer to

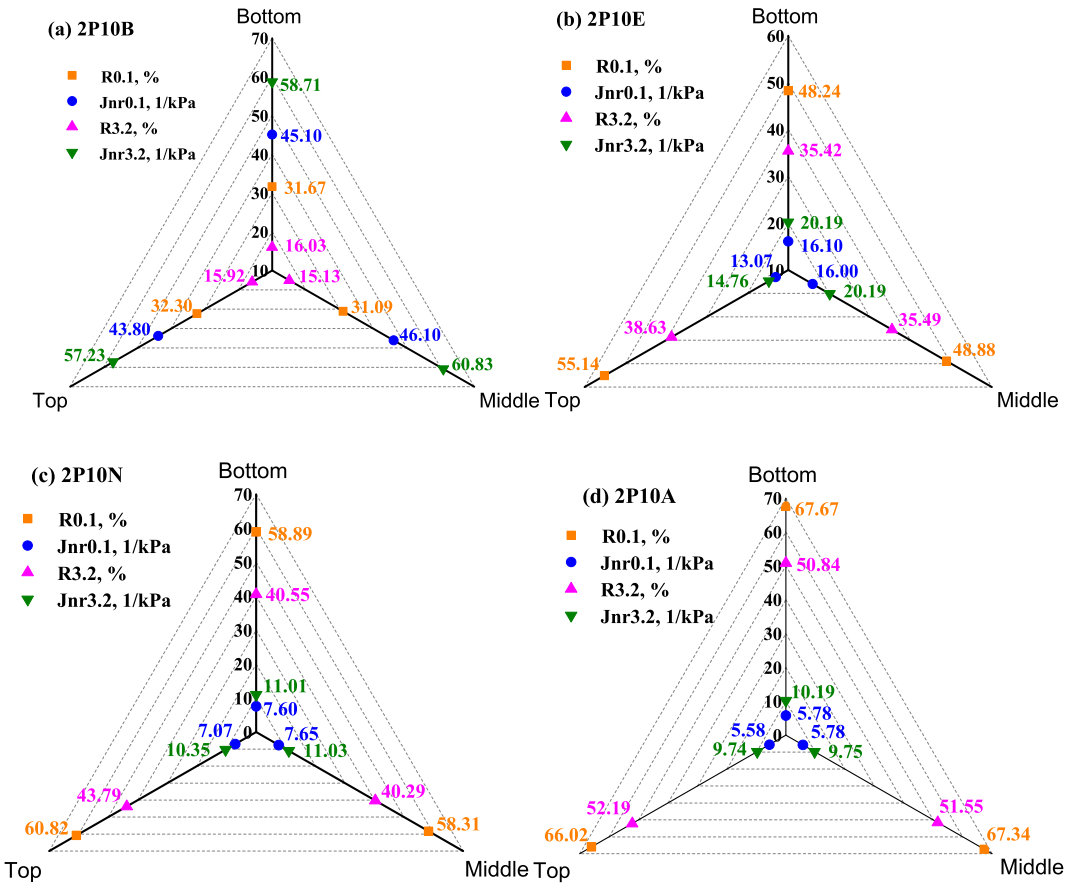

Fig. 17. MSCR results of the bottom, middle, and top samples in rejuvenated binders after the thermal storage at 52℃.

the aromatic structure, carbonyl, and sulfoxide functional groups in aged bitumen after the oxidative aging process. It is manifested that the absorbance strength of the 1600 cm^{-1} peak in aromatic-oil rejuvenated binders is stronger than the others, which is contributed by the polyaromatic structure in aromatic-oil molecules.

The carbonyl index (C═O) and sulfoxide index (S═O) is the most popular chemical signal to evaluate the influence of aging and rejuvenation on the chemical characteristics of bituminous materials, which are calculated as follows:

$$\text{Carbonyl index CI} = \frac{A_{1700}}{\sum A} \tag{15}$$

$$\text{Sulfoxide index SI} = \frac{A_{1030}}{\sum A} \tag{16}$$

where A_{1700} and A_{1030} are the peak area of C═O and S═O functional groups, while $\sum A$ refers to the sum of all peak areas at the wavenumber position of 2952, 2862, 1700, 1600, 1460, 1375, 1030, 864, 814, 743, and 724 cm^{-1}.

In this study, the difference in both carbonyl index and sulfoxide index between the bottom, middle, and top parts of rejuvenated binders after the thermal storage stage and the corresponding separation index values are obtained in Eq. 13 and displayed in Fig. 20. The SI values based on the C═O index are much larger than the S═O index, indicating the former is more sensitive to the phase variation of rejuvenator molecules in aged bitumen during the thermal storage process. According to the SI parameters based on both C═O and S═O indices, the aromatic-oil rejuvenated bitumen shows the lowest SI values and the best thermal storage stability. On the contrary, the engine-oil exhibits the largest separation potential from aged bitumen. It should be mentioned that the ranking result of thermal phase stability for these four rejuvenators from chemical indices is consistent with that from rheological parameters. This finding further confirms the difference in phase stability and compatibility between various rejuvenators in aged binders. Likewise, the negative impacts of the aging level of aged bitumen on the thermal storage stability and compatibility potential between the rejuvenators and aged binders are observed through the SI parameters based on chemical indices.

7. Influence of temperature on compatibility between rejuvenators and aged binders

The high temperature is preferred to strengthen the blending level of rejuvenated bitumen. However, the effects of temperatures on the solubility degree and compatibility between rejuvenators and aged binders are still unclear. Meanwhile, it is difficult to experimentally measure the solubility parameters of rejuvenators and aged binders at different temperatures. In this study, the δ values between the rejuvenators and aged bitumen at different temperatures are outputted from MD simulations, and the corresponding Δδ values are calculated to assess the compatibility potential of various rejuvenators in aged binders with different aging levels and temperatures from the aspect of intermolecular interaction.

Fig. 21 demonstrates the δ values of the virgin, aged bitumen, and four rejuvenators versus the temperature. The increment of aging degree remarkably enlarges the δ values of bitumen, and

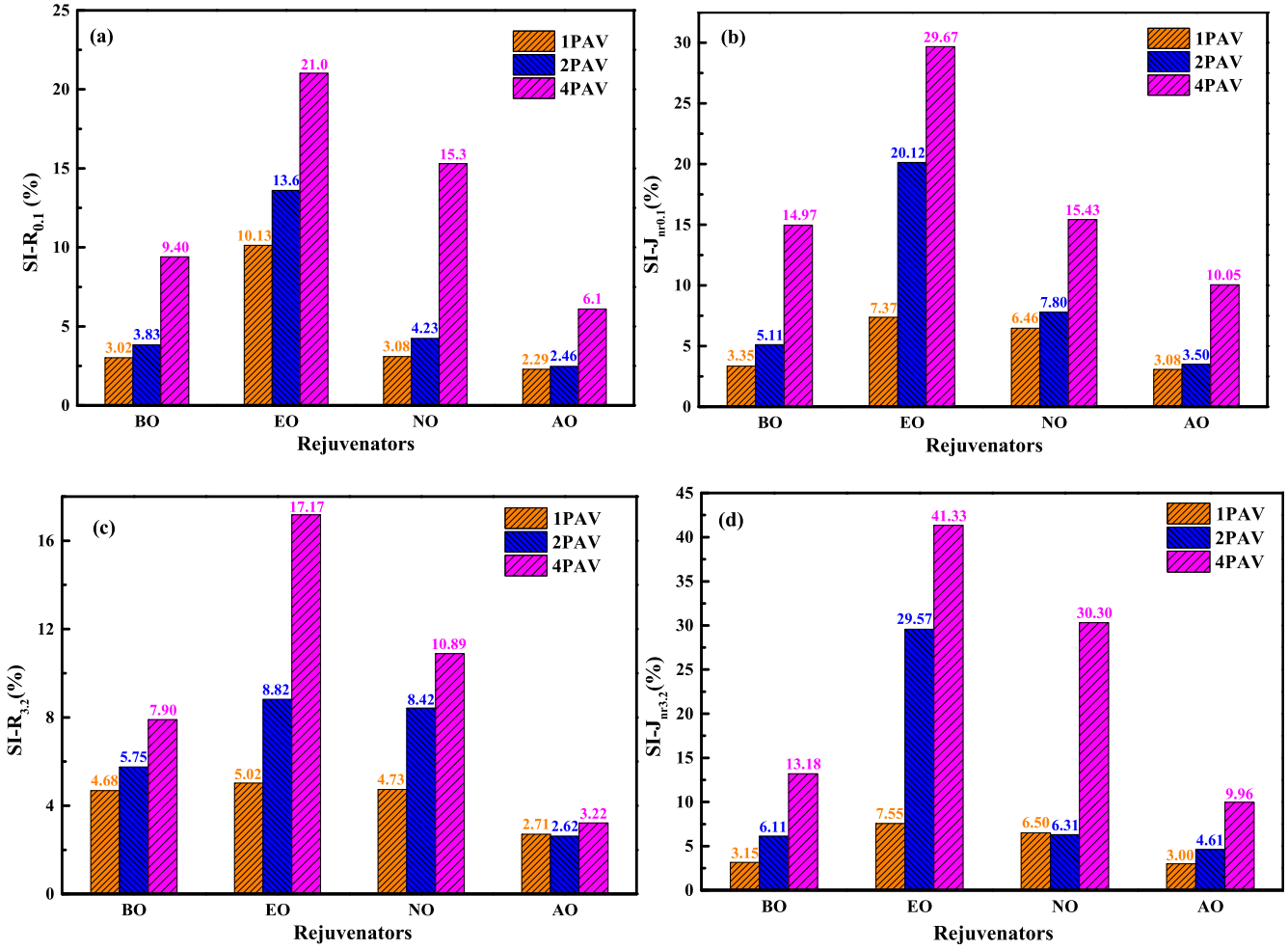

Fig. 18. The separation index SI values of rejuvenated binders based on MSCR parameters of (a) $R_{0.1}$, (b) $J_{nr0.1}$, (c) $R_{3.2}$, and (d) $J_{nr3.2}$.

the ranking of δ values for four rejuvenators at all temperatures is the same as AO > BO > EO > NO. Meanwhile, the δ values of all rejuvenators are lower than all long-term aged binders, indicating their restoration potential on the δ parameters of aged bitumen to the virgin bitumen level. As the temperature rises, the δ values of all bitumen and rejuvenators show a decreasing trend, which is associated with the weakened intermolecular interaction and cohesion energy at high temperatures. That's why the rejuvenators and aged binders can be blended well at high temperatures with enhanced molecular mobility and large intermolecular free volume.

However, the large blending level between rejuvenators and aged bitumen under the high mechanical mixing and high-temperature condition cannot ensure their sufficient compatibility. According to the separation index values during the thermal storage test, the rejuvenated binders show the phase separation potential at a high temperature of 160℃, especially the engine-oil and naphthenic-oil rejuvenated binders. Therefore, the high-temperature condition would accelerate the phase separation of rejuvenators from rejuvenated bitumen because of the high molecular mobility and low intermolecular interaction with aged bitumen molecules. Fig. 22 shows the Δδ parameters between four rejuvenators and aged binders. When the temperature and aging degree of bitumen are fixed, the Δδ values of engine-oil and naphthenic-oil rejuvenated binders are higher than bio-oil rejuvenated bitumen, while the aromatic-oil rejuvenated binders exhibit the lowest Δδ parameters. It implies that the aromatic-oil and bio-oil display a much superior compatible capacity with aged bitumen molecules than the naphthenic-oil and engine-oil rejuvenators.

For all rejuvenated binders, the Δδ values increase distinctly as the aging level of bitumen deepens. It means that the compatibility extent between all rejuvenators and aged bitumen worsens when the more severe aged bitumen is reused. To reduce the phase separation potential, the aromatic-oil and bio-oil rejuvenators are suitable for rejuvenating severely aged bitumen. In contrast, the engine-oil and naphthenic-oil rejuvenators could be used for slightly aged binders. Interestingly, all rejuvenated binders present a higher Δδ value with the increase in temperature. It indicates that the compatibility level between the rejuvenators and aged binders tends to be lower as the temperature increases. The intermolecular interaction between the rejuvenator and aged bitumen molecule is reduced, and their molecular mobility is enhanced, leading to decreasing compatibility. As a result, it is summarized that the high temperatures benefit the increased blending level, but they adversely influence the compatibility and thermal storage stability between the rejuvenators and aged binders. The temperatures selected for various rejuvenators blending should be optimized by balancing the diffusive and compatibility behaviors of these rejuvenators. For example, high temperatures can be chosen for the aromatic-oil rejuvenated bitumen with a low diffusion coefficient but high compatibility capacity. On the contrary, with regard to the engine-oil rejuvenator showing large diffusive capacity but low compacity, a low blending temperature is the first

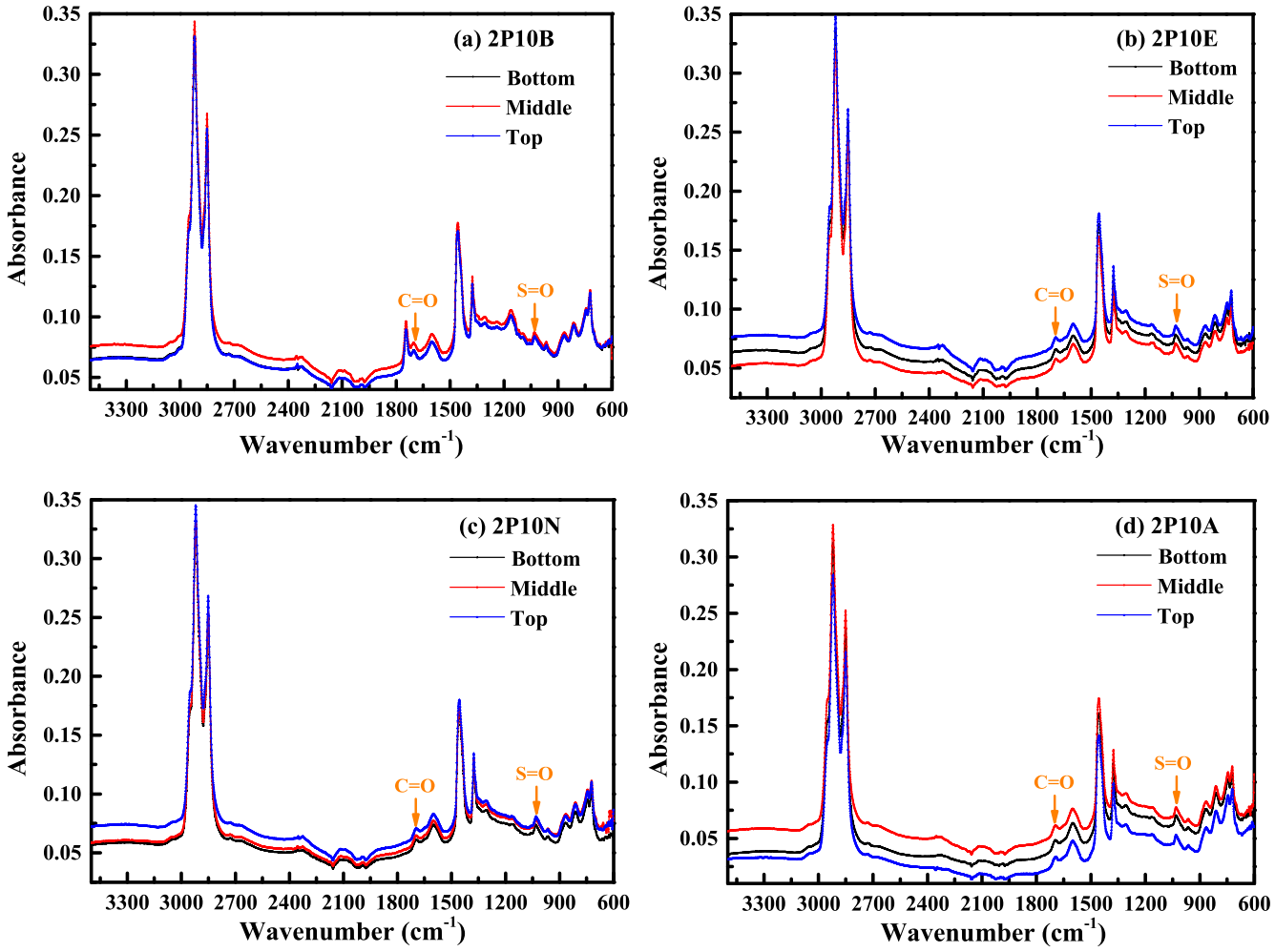

Fig. 19. The FTIR curves of the bottom, middle, and top sections of different rejuvenated binders after the thermal storage process.

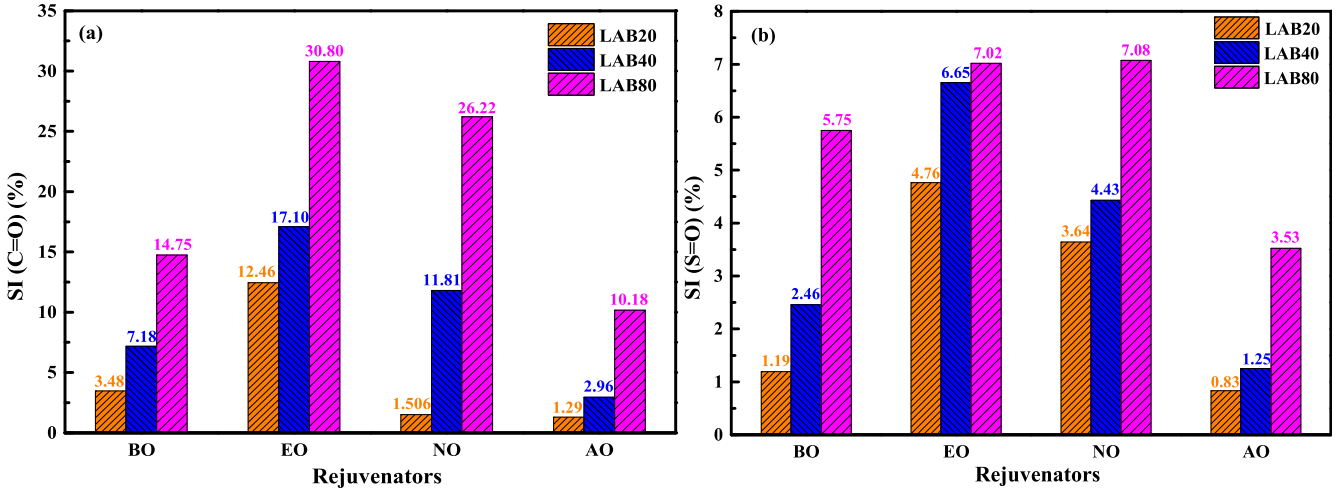

Fig. 20. The separation index SI values of rejuvenated bitumen based on FTIR parameters of carbonyl index C=O and sulfoxide index S=O.

choice. In addition, more efficient rejuvenators with excellent diffusive and compatibility performance (such as bio-oil rejuvenator) should be developed in the future. Lastly, it is necessary to consider the aging degree of bitumen when the blending conditions are determined, which significantly affects the diffusive and compatibility behaviors of rejuvenators.

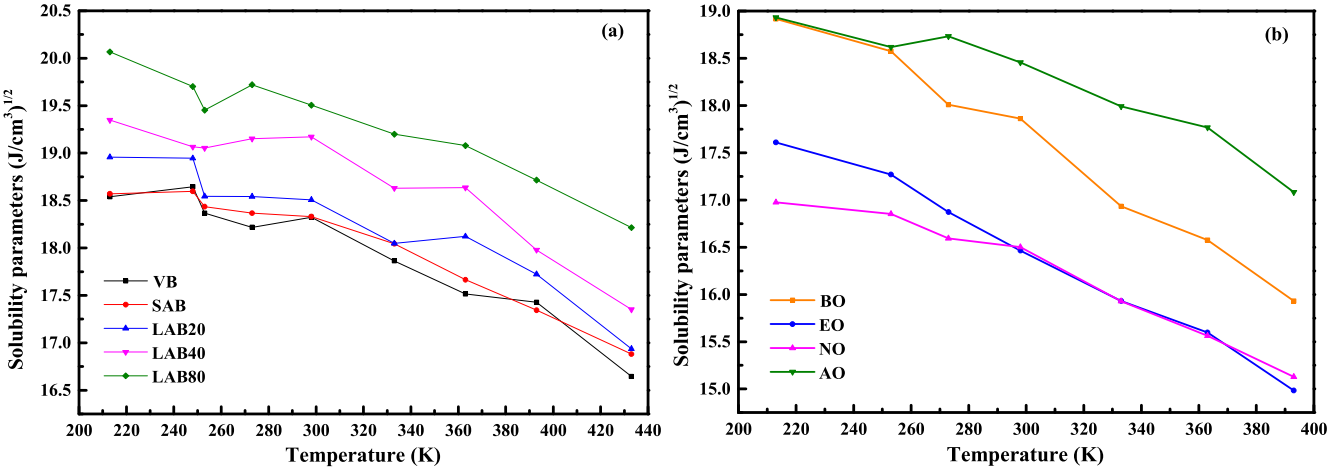

Fig. 21. The solubility parameter values of the virgin, aged bitumen (a), and rejuvenators (b).

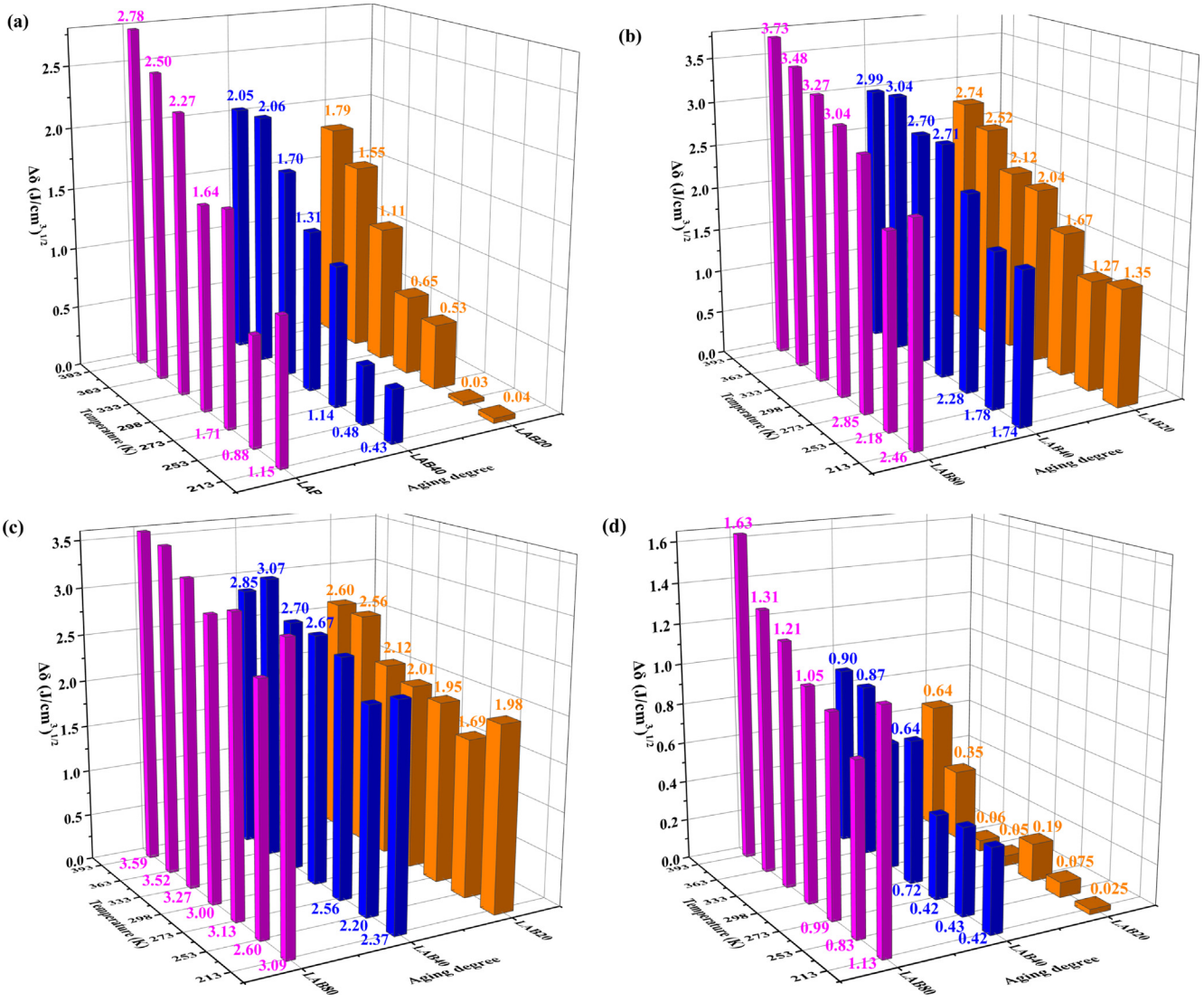

Fig. 22. Influence of temperature on the Δδ values between rejuvenators and aged binders (a) Bio-oil; (b) Engine-oil; (c) Naphthenic-oil; (d) Aromatic-oil.

8. Conclusions and recommendations

The compatibility and thermal phase stability issues of rejuvenators in aged bitumen are complicated, especially at the molecular scale. In this study, different evaluation parameters in terms of thermodynamic parameters, intermolecular binding energy, molecular distribution, and molecular mobility of various rejuvenator molecules are predicted from MD simulations to assess and compare the compatibility behaviors of rejuvenators in aged binders. In addition, the experimental thermal storage tests are implemented on rejuvenated binders to detect the difference in thermal storage stability and compatibility between various rejuvenators in aged binders. The atomic-scale findings from MD simulations explain the complicated underlying mechanism. Furthermore, the influence of bitumen aging degrees and temperature on the compatibility and thermal phase stability of various rejuvenated bitumen systems are also discussed. The main conclusions from this study are listed as follows:

(1) The thermodynamic parameters of $\Delta\delta$, χ, and ΔG_m are efficient in estimating the compatibility potential of various rejuvenators with aged bitumen, and their value ranking for four rejuvenators is the same as EO > NO > BO > AO. It suggests that the compatible capacity of aromatic-oil with aged binders is the largest, followed by the bio-oil and naphthenic-oil rejuvenators, while the engine-oil exhibits the worst compatibility performance.
(2) The intermolecular binding energy $E_{binding}$ values of different rejuvenated bitumen are calculated, and it manifests that the aromatic-oil and engine-oil molecules display the strongest and weakest interaction strength with aged bitumen molecules. The $E_{binding}$ parameter results validate and explain the compatibility predictions based on thermodynamics parameters at the molecular scale.
(3) Various rejuvenators present the different molecular dispersion levels in the rejuvenated bitumen model. The molecular distribution of engine-oil molecules is the most homogeneous, while the aromatic-oil exhibits a worse molecular dispersion condition than the bio-oil and naphthenic-oil rejuvenators.
(4) It is possible for both aromatic-oil and bio-oil molecules to penetrate the asphaltene clusters in aged bitumen, while the naphthenic-oil and engine-oil molecules are mostly dispersed in the aromatic/resin and saturate phase, respectively. Moreover, the ranking of molecular mobility for four rejuvenators in aged bitumen is BO > EO > NO > AO.
(5) From the results of separation index SI values from both rheological and chemical indices, it is demonstrated that the sequence of thermal storage stability four these rejuvenators follows AO > BO > NO > EO, showing the same trend as the compatibility result based on thermodynamics parameters predicted from MD simulations. Meanwhile, the SI values of all rejuvenated binders are dependent on the characterization parameter type.
(6) The increment in the aging degree of bitumen results in the increase of $\Delta\delta$ and SI values, as well as the intermolecular attraction level, while the molecular distribution uniformity and diffusive mobility of rejuvenator molecules are weakened. It suggests that the compatibility and thermal phase stability of rejuvenated bitumen tend to be worse when severely-aged bitumen is reused.
(7) The $\Delta\delta$ results reveal that the high temperature adversely influences the compatibility between rejuvenators and aged binders. Although a high temperature is beneficial to improve the blending degree between rejuvenators and aged bitumen, it would increase the thermal separation potential and uneven distribution of rejuvenator molecules. A high construction temperature suits aromatic-oil rejuvenated bitumen with a low diffusion coefficient but high compatibility level. On the contrary, with regard to the engine-oil rejuvenator showing large diffusive capacity but low compacity, a low blending temperature is the first choice.

Based on the findings from this study, it is demonstrated that the thermal storage stability of rejuvenated binders is strongly affected by rejuvenator type and the aging degree of bitumen, which shows a high correlation with the compatibility prediction from MD simulations. However, the thermal behavior of rejuvenators in aged bitumen is a complicated system composed of intermolecular interaction strength, molecular dispersion, and molecular mobility. Therefore, more work should be conducted on exploring the complex relationship between the compatibility potential from MD simulations and phase stability parameters of rejuvenated bitumen from experimental tests. During the practical rejuvenation process of RAP materials, the blending degree between the rejuvenator and aged binder is determined by the diffusion capacity and compatibility (thermal phase stability) performance of the rejuvenator. These two factors should be coupled in future studies on blending degree investigations of rejuvenated binders. As a result, more efficient rejuvenators with superior diffusion rates and compatibility potential will be developed.

CRediT authorship contribution statement

Shisong Ren: Methodology, Investigation, Formal analysis, Writing – original draft, Writing – review & editing. **Xueyan Liu:** Supervision, Writing – review & editing. **Peng Lin:** Resources, Methodology, Supervision. **Yangming Gao:** Methodology, Supervision. **Sandra Erkens:** Methodology, Supervision.

Data availability

Data will be made available on request.

Declaration of Competing Interest

The authors declare that they have no known competing financial interests or personal relationships that could have appeared to influence the work reported in this paper.

Acknowledgments

The first author would thank the China Scholarship Council for the funding support (CSC. No. 201906450025).

Appendix A. Supplementary data

Supplementary data to this article can be found online at https://doi.org/10.1016/j.matdes.2022.111141.

References

[1] A. Sreeram, Z. Leng, Y. Zhang, R.K. Padhan, Evaluation of RAP binder mobilization and blending efficiency in bituminous mixtures: An approach using ATR-FTIR and artificial aggregate, Constr. Build. Mater. 179 (2018) 245–253.
[2] K. Zhang, H. Wen, A. Hobbs, Laboratory tests and numerical simulations of mixing superheated virgin aggregate with reclaimed asphalt pavement materials, Transp. Res. Rec.: J. Transp. Res. Board 2506 (1) (2015) 62–71.
[3] M.C. Cavalli, M.N. Partl, L.D. Poulikakos, Measuring the binder film residues on black rock in mixtures with high amounts of reclaimed asphalt, J. Cleaner Prod. 149 (2017) 665–672.

[4] S. Yu, S. Shen, C. Zhang, W. Zhang, X. Jia, Evaluation of the blending effectiveness of reclaimed asphalt pavement binder, J. Mater. Civ. Eng. 29 (12) (2017) 04017230.
[5] P. Lin, X. Liu, P. Apostolidis, S. Erkens, S. Ren, S. Xu, T. Scarpas, W. Huang, On the rejuvenator dosage optimization for aged SBS modified bitumen, Constr. Build. Mater. 271 (2021) 121913.
[6] R. Tauste, F. Moreno-Navarro, M. Sol-Sanchez, M.C. Rubio-Gamez, Understanding the bitumen ageing phenomenon: A review, Constr. Build. Mater. 192 (2018) 593–609.
[7] P. Apostolidis, X. Liu, C. Kasbergen, A. Scarpas, Synthesis of asphalt binder aging and the state of the art of anti-aging technologies, Transp. Res. Rec.: J. Transp. Res. Board 2633 (2017) 147–153.
[8] S. Zhang, Y. Cui, W. Wei, Low-temperature characteristics and microstructure of asphalt under complex aging conditions, Constr. Build. Mater. 303 (2021) 124408.
[9] F. Li, Y. Wang, K. Zhao, The hierarchical structure of bitumen of different aging states at the molecular level and nanoscale, Fuel 319 (2022) 123791.
[10] A. Behood, Application of rejuvenators to improve the rheological and mechanical properties of asphalt binders and mixtures: A review, J. Cleaner Prod. 231 (2019) 171–182.
[11] X. Han, S. Mao, S. Xu, Z. Cao, S. Zeng, J. Yu, Development of novel composite rejuvenators for efficient recycling of aged SBS modified bitumen, Fuel 318 (2022) 123715.
[12] S. Xu, X. Liu, A. Tabakovic, P. Lin, Y. Zhang, S. Nahar, B.J. Lommerts, E. Schlangen, The role of rejuvenators in embedded damage healing for asphalt pavement, Mater. Des. 202 (2021) 109564.
[13] M. Guo, A. Motamed, Y. Tan, A. Bhasin, Investigating the interaction between asphalt binder and fresh and simulated RAP aggregate, Mater. Des. 105 (2016) 25–33.
[14] A. Sreeram, Z. Leng, R. Hajj, W.L.G. Ferreira, Z. Tan, A. Bhasin, Fundamental investigation of the interaction mechanism between new and aged binders in binder blends, Int. J. Pavement Eng. (2020), https://doi.org/10.1080/10298436.2020.1799208.
[15] S. Vassaux, V. Gaudefroy, L. Boulange, L.J. Soro, A. Pevere, A. Michelet, V. Barragan-Montero, V. Mouillet, Study of remobilization phenomena at reclaimed asphalt binder/virgin binder interphases for recycled asphalt mixtures using novel microscopic methodologies, Constr. Build. Mater. 165 (2018) 846–858.
[16] F. Kaseer, E. Arambula-Mercado, A.E. Martin, A method to quantify reclaimed asphalt pavement binder availability (effective RAP binder) in recycled asphalt mixes, Transp. Res. Rec. 2673 (1) (2019) 205–216.
[17] M. Oreskovic, G.M. Pires, S. Bressi, K. Vasconcelos, D.L. Presti, Quantitative assessment of the parameters linked to the blending between reclaimed asphalt binder and recycling agent: A literature review, Constr. Build. Mater. 234 (2020) 117323.
[18] C. Castorena, S. Pape, C. Mooey, Blending measurements in mixtures with reclaimed asphalt, Transp. Res. Rec.: J. Transp. Res. Board 2574 (2016) 57–63.
[19] S. Zhao, B. Bowers, B. Huang, X. Shu, Characterizing rheological properties of binder and blending efficiency of asphalt paving mixtures containing RAS through GPC, J. Mater. Civ. Eng. 26 (5) (2014) 941–946.
[20] D.L. Presti, K. Vasconcelos, M. Oreskovic, G.M. Pires, S. Bressi, On the degree of binder activity of reclaimed asphalt and degree of blending with recycling agents, Road Mater. Pavement Des. 21 (8) (2020) 2071–2090.
[21] S. Zhao, B. Huang, X. Shu, M.E. Woods, Quantitative evaluation of blending and diffusion in high RAP and RAS mixtures, Mater. Des. 89 (2016) 1161–1170.
[22] P. Shirodkar, Y. Mehta, A. Nolan, K. Sonpal, A. Norton, C. Tomlinson, E. Dubois, P. Sullivan, R. Sauber, A study to determine the degree of partial blending of reclaimed asphalt pavement (RAP) binder for high RAP hot mix asphalt, Constr. Build. Mater. 25 (2011) 150–155.
[23] M. Mohajeri, A.A.A. Molenaar, M.F.C. Van de Ven, Experimental study into the fundamentally understanding of blending between reclaimed asphalt binder and virgin bitumen using nanoindentation and nano-computed tomography, Road Mater. Pavement Des. 15 (2) (2014) 372–384.
[24] A. Margaritis, G. Tofani, G. Jacobs, J. Blom, S. Tavernier, C. Vuye, W., Van den bergh. On the applicability of ATR-FTIR microscopy to evaluate the blending between neat bitumen and bituminous coating of reclaimed asphalt, Coatings. 9 (2019) 240.
[25] P. Shirodkar, Y. Mehta, A. Nolan, E. Dubois, D. Reger, L. McCarthy, Development of blending chart for different degrees of blending of RAP binder and virgin binder, Resour. Conserv. Recycl. 73 (2013) 156–161.
[26] F.Y. Rad, N.R. Sefidmazgi, H. Bahia, Application of diffusion mechanism: degree of blending between fresh and recycled asphalt pavement binder in dynamic shear rheometer, Transp. Res. Rec.: J. Transp. Res. Board 2444 (2014) 71–77.
[27] P. Kriz, D.L. Grant, B.A. Veloza, M.J. Gale, A.G. Blahey, J.H. Brownie, R.D. Shirts, S. Maccarrone, Blending and diffusion of reclaimed asphalt pavement and virgin asphalt binders, Road Mater. Pavement Des. 15 (S1) (2014) 78–112.
[28] Y. Ding, B. Huang, X. Shu, Characterizing blending efficiency of plant produced asphalt paving mixtures containing high RAP, Constr. Build. Mater. 126 (2016) 172–178.
[29] W.S. Mogawer, A. Booshehrian, S. Vahidi, A.J. Austerman, Evaluating the effect of rejuvenators on the degree of blending and performance of high RAP, RAS, and RAP/RAS mixtures, Road Mater. Pavement Des. 14 (S2) (2013) 193–213.
[30] B. Cui, X. Gu, D. Hu, Q. Dong, A Multiphysics evaluation of the rejuvenator effects on aged asphalt using molecular dynamics simulations, J. Cleaner Prod. 259 (2020) 120629.
[31] Y. Ding, M. Deng, X. Cao, M. Yu, B. Tang, Investigation of mixing effect and molecular aggregation between virgin and aged asphalt, Constr. Build. Mater. 221 (2019) 301–307.
[32] M. Su, J. Zhou, J. Lu, W. Chen, H. Zhang, Using molecular dynamics and experiments to investigate the morphology and micro-structure of SBS modified asphalt binder, Mater. Today Commun. 30 (2022) 103082.
[33] C. Yu, K. Hu, Q. Yang, D. Wang, W. Zhang, G. Chen, C. Kapyelata, Analysis of the storage stability property of carbon nanotube/recycled polyethylene-modified asphalt using molecular dynamics simulations, Polymers. 13 (2021) 1658.
[34] M. Li, Z. Min, Q. Wang, W. Huang, Z. Shi, Effect of epoxy resin content and conversion rate on the compatibility and component distribution of epoxy asphalt: A MD simulation study, Constr. Build. Mater. 319 (2022) 126050.
[35] J. Zhu, R. Balieu, H. Wang, The use of solubility parameters and free energy theory for phase behavior of polymer-modified bitumen: a review, Road Mater. Pavement Des. (2019), https://doi.org/10.1080/14680629.2019.1645725.
[36] A. Jarray, V. Gerbaud, M. Hemati, Polymer-plasticizer compatibility during coating formulation: A multi-scale investigation, Prog. Org. Coat. 101 (2016) 195–206.
[37] A. Takhulee, Y. Takahashi, V. Vao-soongnern, Molecular simulation and experimental studies of the miscibility of polylactic acid/polyethylene glycol blends, J. Polym. Res. 24 (2017) 8.
[38] X. Zhang, Y. Ning, X. Zhou, X. Xu, X. Chen, Quantifying the rejuvenation effects of soybean-oil on aged asphalt-binder using molecular dynamics simulations, J. Cleaner Prod. 317 (2021) 128375.
[39] NCAT, NCAT Researchers Explore Multiple User of rejuvenators asphalt technology news. 2014, 26 (NO.1 Spring), 1-16
[40] S. Ren, X. Liu, P. Lin, R. Jing, S. Erkens, Toward the long-term aging influence and novel reaction kinetics models of bitumen, Int. J. Pavement Eng. http://doi.org/10.1080/10298436.2021.2024188.
[41] D. Oldham, A. Rajib, K.P.R. Dandamudi, Y. Liu, S. Deng, E.H. Fini, Transesterification of waste cooking oil to produce a sustainable rejuvenator for aged asphalt, Resour. Conserv. Recycl. 168 (2021) 105297.
[42] EN 15326. British standard for bitumen and bituminous binders-measurement of density and specific gravity-capillary-stoppered pycnometer method.
[43] H. Wang, X. Liu, S. Erkens, A. Skarpas, Experimental characterization of storage stability of crumb rubber modified bitumen with warm-mix additives, Constr. Build. Mater. 249 (2020) 118840.
[44] S. Ren, X. Liu, M. Li, W. Fan, J. Xu, S. Erkens, Experimental characterization of viscoelastic behaviors, microstructure and thermal stability of CR/SBS modified asphalt with TOR, Constr. Build. Mater. 261 (2020) 120524.
[45] S. Ren, M. Liang, W. Fan, Y. Zhang, C. Qian, Y. He, J. Shi, Investigating the effects of SBR on the properties of gilsonite modified asphalt, Constr. Build. Mater. 190 (2018) 1103–1116.
[46] AASHTO M320. Standard specification for performance-graded asphalt binder.
[47] AASHTO TP70. Standard method of test for multiple stress creep recovery (MSCR) test of asphalt binder using a Dynamic Shear Rheometer (DSR), American Association of State Highway and Transportation Officials, Washington (DC), 2009.
[48] D.D. Li, M.L. Greenfield, Chemical compositions of improved model asphalt systems for molecular simulations, Fuel 115 (2014) 347–356.
[49] S. Ren, X. Liu, P. Lin, S. Erkens, Y. Xiao, Chemo-physical characterization and molecular dynamics simulation of long-term aging behaviors of bitumen, Constr. Build. Mater. 302 (2021) 124437.
[50] G. Xu, H. Wang, Molecular dynamics study of oxidative aging effect on asphalt binder properties, Fuel 188 (2017) 1–10.
[51] D. Hu, X. Gu, B. Cui, J. Pei, Q. Zhang, Modeling the oxidative aging kinetics and pathways of asphalt: A ReaxFF molecular dynamics study, Energy Fuels 34 (3) (2020) 3601–3613.
[52] Y. Yang, Y. Wang, J. Cao, Z. Xu, Y. Li, Y. Liu, Reactive molecular dynamic investigation of the oxidative aging impact on asphalt, Constr. Build. Mater. 279 (2021) 121298.
[53] S. Ren, X. Liu, P. Lin, Y. Gao, S. Erkens, Molecular dynamics simulation on bulk bitumen systems and its potential connections to macroscale performance: Review and discussion, Fuel 328 (2022) 125382.
[54] S. Ren, X. Liu, P. Lin, S. Erkens, Y. Gao, Y. Xiao, Chemical characterizations and molecular dynamics simulations on different rejuvenators for aged bitumen recycling, Fuel 324 (2022) 124550.
[55] A. Sceeram, Z. Leng, R. Hajj, A. Bhasin, Characterization of compatibility between aged and unaged binders in bituminous mixtures through an extended HSP model of solubility, Fuel 254 (2019) 115578.
[56] Y. Luo, R. Wang, W. Wang, L. Zhang, S. Wu, Molecular dynamics simulation insight into two-component solubility parameters of graphene and thermodynamic compatibility of graphene and styrene butadiene rubber, J. Phys. Chem. C 121 (2017) 10163–10173.
[57] H.F. Haghshenas, R. Rea, G. Reinke, M. Zaumanis, E.H. Fini, Relationship between colloidal index and chemo-rheological properties of asphalt binders modified by various recycling agents, Constr. Build. Mater. 318 (2022) 126161.
[58] M. Elkashef, D. Jones, L. Jiao, R.C. Williams, J. Harvey, Using thermal analytical techniques to study rejuvenators and rejuvenated reclaimed asphalt pavement binders, Energy Fuels 33 (2019) 2651–2658.
[59] P. Wang, Z. Dong, Y. Tan, Z. Liu, Investigating the interactions of the saturate, aromatic, resin, and asphaltene four fractions in asphalt binders by molecular simulations, Energy Fuels 29 (2015) 112–121.

[60] J. Zhang, X. Gong, G. Wang, Compatibility and mechanical properties of BAMO-AMMO/DIANP composites: A molecular dynamics simulation, Comput. Mater. Sci. 102 (2015) 1–6.
[61] G. Li, Y. Tan, The construction and application of asphalt molecular model based on the quantum chemistry calculation, Fuel 308 (2022) 122037.
[62] H.F. Haghshenas, R. Rea, G. Reinke, D.F. Haghshenas, Chemical characterization of recycling agents, J. Mater. Civ. Eng. 32 (5) (2020) 0602005.
[63] X. Yang, J. Mills-Beale, Z. You, Chemical characterization and oxidative aging of bio-asphalt and its compatibility with petroleum asphalt, J. Cleaner Prod. 142 (2017) 1837–1847.